

| | |
|---------------------|---|
| Zeitschrift: | IABSE congress report = Rapport du congrès AIPC = IVBH Kongressbericht |
| Band: | 10 (1976) |
| Rubrik: | Theme Ib: Achievements of safety and economy in design and construction |

Nutzungsbedingungen

Die ETH-Bibliothek ist die Anbieterin der digitalisierten Zeitschriften auf E-Periodica. Sie besitzt keine Urheberrechte an den Zeitschriften und ist nicht verantwortlich für deren Inhalte. Die Rechte liegen in der Regel bei den Herausgebern beziehungsweise den externen Rechteinhabern. Das Veröffentlichen von Bildern in Print- und Online-Publikationen sowie auf Social Media-Kanälen oder Webseiten ist nur mit vorheriger Genehmigung der Rechteinhaber erlaubt. [Mehr erfahren](#)

Conditions d'utilisation

L'ETH Library est le fournisseur des revues numérisées. Elle ne détient aucun droit d'auteur sur les revues et n'est pas responsable de leur contenu. En règle générale, les droits sont détenus par les éditeurs ou les détenteurs de droits externes. La reproduction d'images dans des publications imprimées ou en ligne ainsi que sur des canaux de médias sociaux ou des sites web n'est autorisée qu'avec l'accord préalable des détenteurs des droits. [En savoir plus](#)

Terms of use

The ETH Library is the provider of the digitised journals. It does not own any copyrights to the journals and is not responsible for their content. The rights usually lie with the publishers or the external rights holders. Publishing images in print and online publications, as well as on social media channels or websites, is only permitted with the prior consent of the rights holders. [Find out more](#)

Download PDF: 08.08.2025

ETH-Bibliothek Zürich, E-Periodica, <https://www.e-periodica.ch>

Dynamic Design Criteria for Tall Buildings in Japan

Critères dynamiques pour le calcul de bâtiments de grande hauteur au Japon

Dynamische Entwurfskriterien für Hochhäuser in Japan

KIYOSHI MUTO

Member, Japan Academy
Vice-President, Kajima Corporation
Tokyo, Japan

MASAYUKI NAGATA

Senior Research Engineer
Muto Institute of Structural Mechanics
Tokyo, Japan

1. Introduction

The earthquake resistant design is most important in the structural safety in Japan. The design of low buildings under 45 meters are performed by the conventional static method based on "Seismic Co-efficient" method, that is, percent G method.

On the other hand, a unique "Dynamic Design Method" has been established for the high-rise buildings over the height of 45 meters. The procedure of this new method is shown in Fig.1. In this method, the dynamic response analyses are conducted with the aid of a computer using observed records of strong earthquakes as input waves. The strength and deformation of the structure are checked covering the elastic and elastic-plastic ranges, and if the results on stress and strain do not satisfy the design criteria established by the designers to control response stresses and/or deformations, the structural design must be revised and checked again. This procedure is the so-called "feed-back" system.

This paper presents the dynamic design criteria in this procedure and the earthquake response values of several examples.

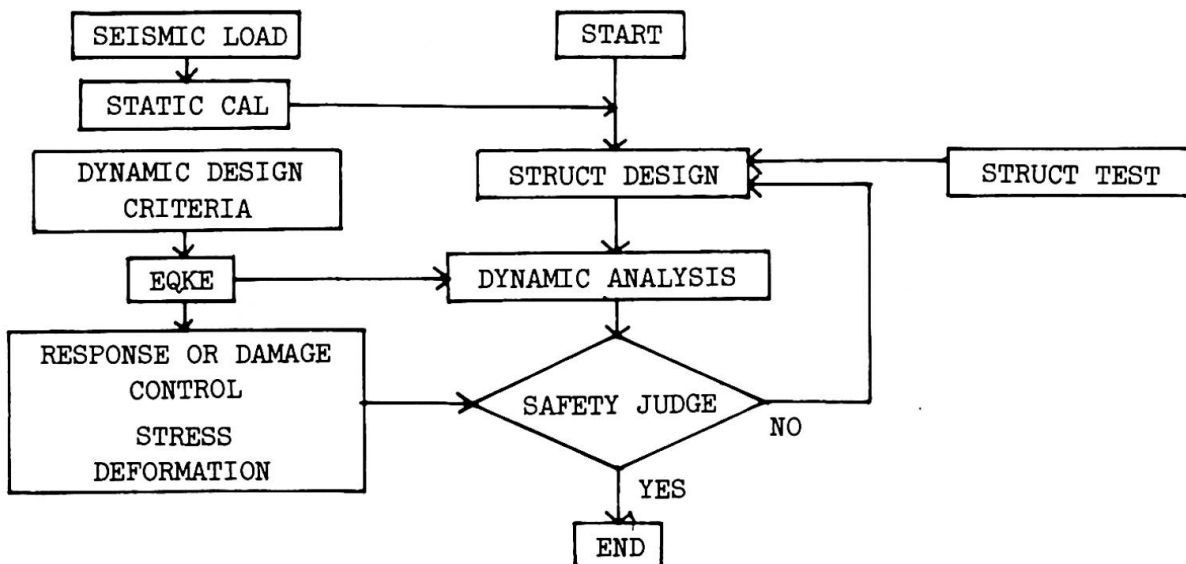


Fig.1 Dynamic Design Procedure of High-rise Building

2. Dynamic Design Criteria

Fig.2 shows the earthquake resistant design criteria set up by the authors' institute. Three degrees of earthquake intensity are assumed and against each degree, response limitations are respectively established.

For a minor or moderate earthquake, categorized as Class I, which occurs after and during which the behaviors of the structure can be confirmed by vibrations tests, the vibration must be controlled to be as small as possible to give no disturbance or discomfort to human. In other words, a high stiffness should be given to the structure in order to minimize the deformation. When an expected severe earthquakes hit, the stresses on all members of the structure must be less than the allowable values and also the secondary members should maintain safe condition. This category level, Class II, may be considered to correspond to the conventional code design level.

In the worst earthquake, hypothetically assumed as Class III, the structural and secondary members may exceed the elastic limit and suffer some damage but must not be severely damaged or collapse.

For the Tokyo region the authors usually assume the maximum acceleration of 0.2 - 0.3G as the Class II earthquake and 0.4 - 0.5G as the Class III earthquake.

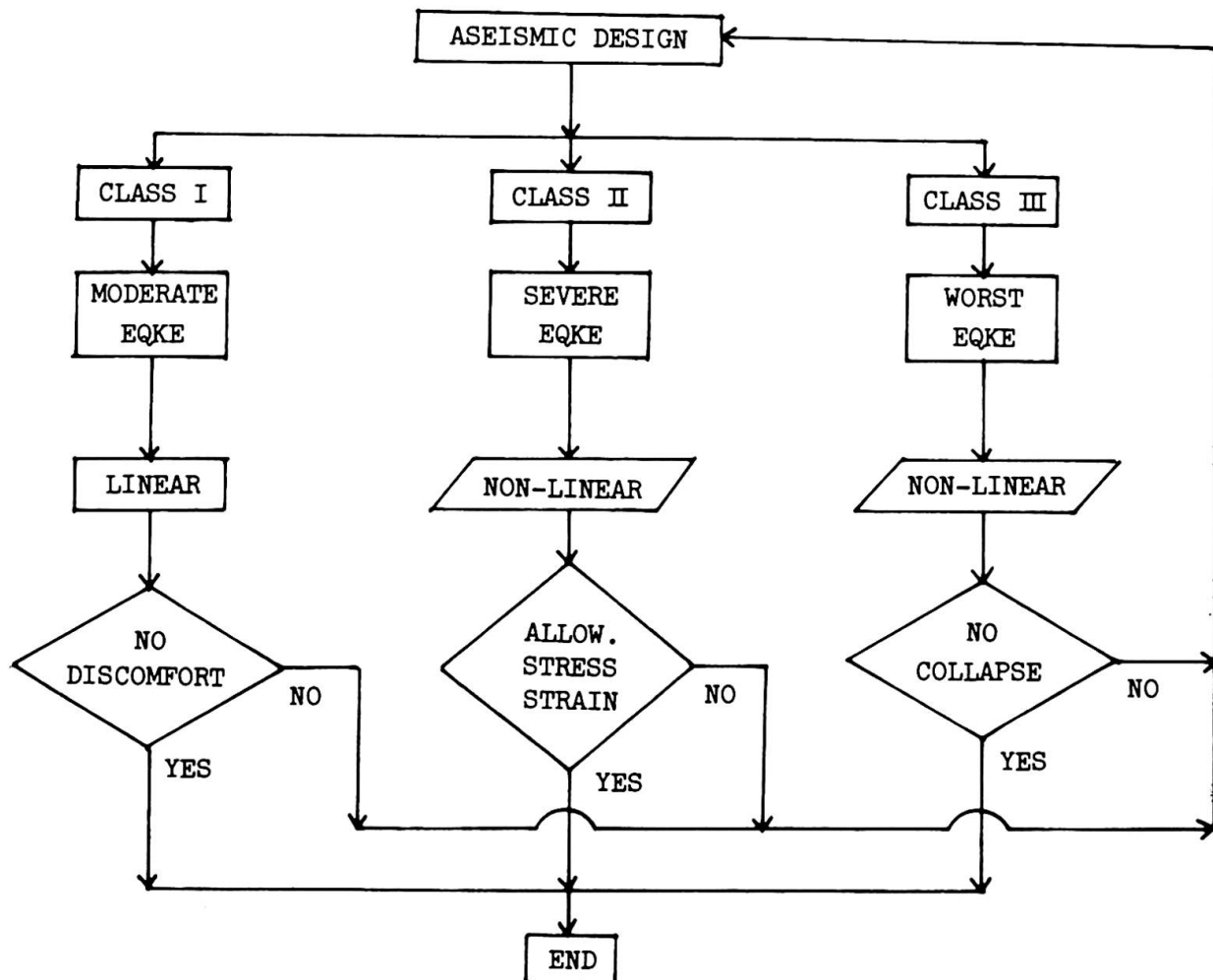


Fig.2 Dynamic Design Criteria Set Up by the Authors' Institute

3. Earthquake Response Values

The authors have undertaken to design and analyze many tall buildings in the way described above. In order to show the damage control, examples of maximum earthquake response values of three buildings are listed in Table 1.

The 60-story office building is under construction in Ikebukuro Subcenter of Tokyo and will be the tallest in Japan. (Photo 1) The earthquake resisting system of this building consists of rigidly connected steel framings with the special ductile reinforced concrete shear walls (slitted wall) as shown in Fig.3. Next 17-story office building consists of steel moment resisting framings only.

For these two high-rise buildings, the authors have assumed the maximum acceleration of 0.25G as the Class II earthquakes and 0.4G as the Class III ones in consideration of the important factor. All of these response values shown in Table 1 are appropriate for the design criteria.

Photo 2 shows the 4-story reinforced concrete garage building. Although the design of this building is in the category in which only the stress check is regulated by the conventional code, the dynamic analysis was performed especially in order to investigate the safety against earthquakes.

In this case the design criteria for tall building are not satisfied, but this building was designed to have sufficient ductility by placement of rebars in special arrangement shown in Fig.4.

Table 1 clarifies that for tall buildings the important problem in designing is the stiffness control, and consequently the tall buildings are given more than sufficient strength. On the other hand for low buildings it is important to control the deformability with satisfactory ductility as much as the strength.

| Building (Structure) | Earthquake Intensity | Damage Control (Max. Value) | | |
|--|-------------------------|-----------------------------|----------------------|---------------------|
| | | Strength | Story Defl. Angle | Ductility Factor |
| 60-story Office (Steel framing & R.C. Slitted Shear Wall) | 0.25G | Elastic | 1/400 | 0.7 |
| | 0.40G | Partially Yield | 1/260 | 1.3 |
| 17-story Office (Steel framing) | 0.25G | Elastic | 1/190 | 0.9 |
| | 0.40G | Partially Yield | 1/110 | 1.4 |
| 4-story Garage (Moment Resisting R.C. framing) | 0.20G | Yield | 1/130 | 1.3 |
| | 0.40G | Yield | 1/60 | 2.6 |

Table 1. Examples of Damage Control

Photo 1. Ikebukuro Subcenter Development (Right: 60-Story Office)

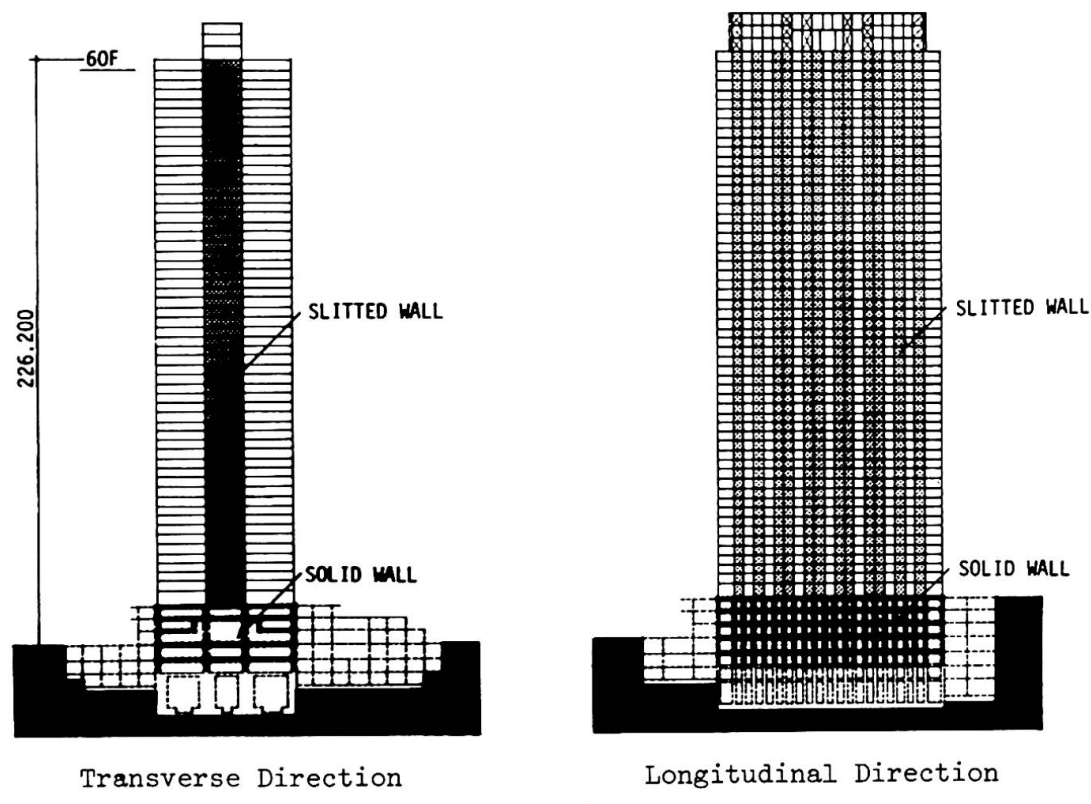


Fig.3 Framing Sections of 60-Story Office Building

Photo 2. 4-Story Reinforced Concrete Garage Building

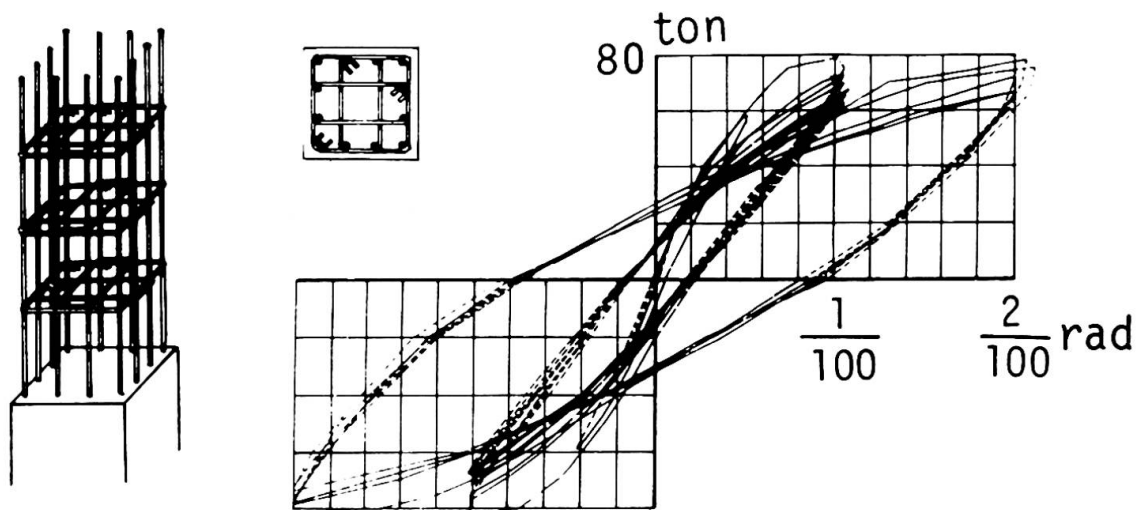


Fig.4 Shear-Deflection Hysteresis Loop of Tied Column
Used in the 4-Story Garage Building

SUMMARY

The feed-back dynamic design system has been accepted in Japan as the most advanced of its kind for tall buildings over 45 meters. In this system dynamic design criteria are indispensable in order to evaluate the earthquake response values obtained from the dynamic analysis. Without those damage evaluations and controls, seismic design, in the true sense of the word, can never be established.

RESUME

La méthode dynamique par itérations successives est, au Japon, reconnue comme la plus avancée pour l'étude des bâtiments de plus de 45 mètres de hauteur. La connaissance des critères dynamiques pour le calcul est indispensable afin d'évaluer les réponses sismiques obtenues par l'analyse dynamique. Sans évaluation des dégâts et sans contrôle, une étude parasismique, au sens propre du terme, ne pourra jamais être mise sur pied.

ZUSAMMENFASSUNG

Die iterative dynamische Berechnungsmethode wurde in Japan als die fortschrittlichste Methode bei Hochhäusern über 45 m angenommen. In dieser Methode ist die Kenntnis der dynamischen Kriterien für die Berechnung unerlässlich, um die Wirkung des Erdbebens nach der dynamischen Analyse abzuschätzen. Ohne diese Schadenermittlungen und Kontrollen ist eine seismische Berechnung und Bemessung undenkbar.

Leere Seite
Blank page
Page vide

Considérations sur la sécurité par rapport à différents types de comportements

Sicherheitsbetrachtungen mit Rücksicht auf verschiedene Verhaltenstypen

Considerations on Safety in Relation to Different Types of Behaviour

D. FRANGOPOL
Assistant
Institut des Constructions
Bucarest, Roumanie

J-C. DOTREPPE
Chargé de Recherches au F.N.R.S.
Université de Liège
Liège, Belgique

1. INTRODUCTION

Dans notre contribution au Rapport Préliminaire [1], nous avons examiné, du point de vue probabiliste, deux types de comportements structuraux : le comportement du type "chaîne" et le comportement du type ductile. Les raisonnements ont été effectués à partir de modèles très schématiques, qui ne permettent de couvrir qu'une gamme assez restreinte de problèmes. C'est le cas, par exemple, de l'étude de la sécurité des structures isostatiques où la ruine d'un élément amène la ruine de l'ensemble de la structure (comportement schématisé par le modèle série - figure 1.-), et de l'étude de la sécurité des structures hyperstatiques dans lesquelles se produit une adaptation plastique entre toutes les sections critiques avant la ruine (comportement schématisé par le modèle parallèle ductile - figure 2.-).



Figure 1

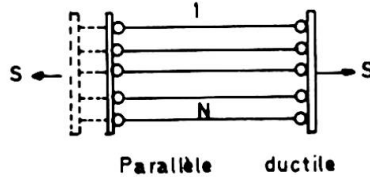
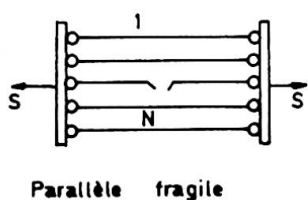


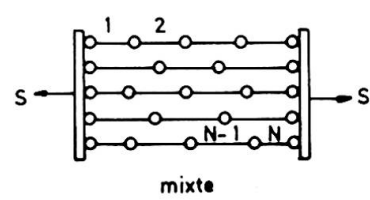
Figure 2

L'objet de cette discussion est de mettre en évidence l'existence d'autres modèles permettant d'étudier la sécurité de constructions dont le comportement est plus complexe, et de présenter un certain nombre de considérations sur ces modèles.

Parmi ceux-ci, on peut citer le modèle parallèle fragile (figure 3), et le modèle mixte (figure 4) constitué par l'association de capacités portantes, en partie en série et en partie en parallèle.



Parallèle fragile



mixte

Figure 3

Figure 4

2. COMPORTEMENT DU TYPE PARALLELE FRAGILE.

Ce type de comportement est caractéristique des constructions hyperstatiques dont les sections ne possèdent pas de capacité de déformation plastique avant la ruine, comme par exemple les structures en béton précontraint. La rupture d'un élément n'engendre pas la ruine d'ensemble de la structure, mais amène une majoration des efforts dans les éléments restants et conduit, par conséquent, à une diminution de la probabilité de survie de ces éléments.

Une des difficultés de l'évaluation de la probabilité globale de survie de la structure réside dans le fait qu'on doit utiliser la théorie des probabilités conditionnelles et considérer l'ensemble des chemins conduisant à la ruine de la structure ("failure paths").

La survie du modèle exige la survie à tous les $N!$ chemins de ruine possibles. La probabilité globale de survie du modèle parallèle fragile (voir figure 3) s'écrit donc [4], [8] :

$$P_{(+)} = P \left(\bigcap_{i=1}^{N!} E_{(+i)} \right) \quad (1)$$

où $E_{(+i)}$ représente l'événement survie par rapport au i -ème chemin de rupture

$N!$ représente le nombre total de chemins de ruine possibles

La probabilité d'apparition du i -ème chemin de ruine, qui pourrait, par exemple, être constitué par la rupture des éléments dans l'ordre 1, 2, 3, ..., N , est donnée par l'expression suivante :

$$P_{(-i)} = P_{(-i)}^{(1)} \cdot P_{(-i)}^{(2/1)} \cdot \dots \cdot P_{(-i)}^{(k/1, 2, \dots, k-1)} \cdot P_{(-i)}^{(N/1, 2, \dots, N-1)} \quad (2)$$

où $P_{(-i)}^{(k/1, 2, \dots, k-1)}$ représente la probabilité (conditionnelle) de rupture du k -ème élément dans le i -ème chemin de ruine, étant donné que les $k-1$ éléments précédents se sont déjà rompus.

Les inégalités suivantes :

$$P_{(-i)}^{(1)} < P_{(-i)}^{(2/1)} < \dots < P_{(-i)}^{(N/1, 2, \dots, N-1)} \quad (3)$$

sont évidemment respectées.

Dans le cas général, le calcul analytique de $P_{(+)}$ s'avère difficile. On se bornera ici à encadrer la probabilité globale de survie par deux nombres plus simples à calculer [5], [6] :

$$\prod_{i=1}^{N!} P_{(+i)} \leq P_{(+)} \leq \min_{i=1}^{N!} (P_{(+i)}) \quad (4)$$

Il faut noter que la probabilité donnée par la borne inférieure se trouve du côté de la sécurité. Elle s'obtient en supposant que les $N!$ chemins sont statistiquement indépendants. Cette probabilité sera d'autant plus proche de $P_{(+)}^o$ que la corrélation entre les chemins de ruine sera faible.

En supposant les N éléments identiques et en imposant que la probabilité de survie du modèle $P_{(+)}^o$ soit au moins égale à une valeur de référence $P_{(+)}^o$ acceptée a priori, on peut écrire la relation :

$$P_{(+)}^o = (P_{(+)}^o)^N$$

Une relation simple peut aussi être établie en ce qui concerne les probabilités de ruine :

$$P_{(-)}^o = 1 - P_{(+)}^o = 1 - (1 - P_{(-)}^o)^N \approx N! P_{(-)}^o$$

3. BREVE COMPARAISON ENTRE LES MODELES SERIE, PARALLELE FRAGILE ET PARALLELE DUCTILE.

3.1. Pour illustrer cette comparaison, on considère l'exemple simple d'une poutre encastrée-appuyée soumise à une charge concentrée P (figure 5.a). La poutre possède deux sections potentiellement critiques 1 et 2.

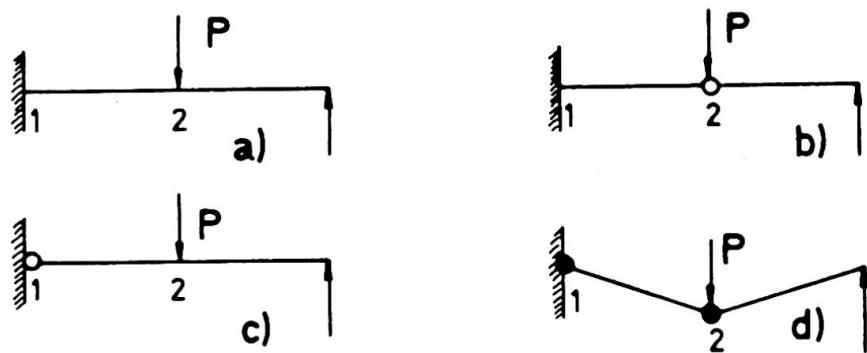


Figure 5

- a) Lorsqu'on applique le concept du dimensionnement élastique, le modèle de comportement est, du point de vue probabiliste, un modèle série. Dans ce cas en effet, on considère que la structure est mise hors service quand on atteint la sollicitation maximum admissible dans la section 1 ou dans la section 2.
- b) On considère à présent comme état-limite l'effondrement du système et on suppose que le matériau a un comportement du type fragile (sections à très faible ductilité). Dans ce cas, on peut définir deux chemins de ruine tout à fait distincts :
 - la poutre cède d'abord en 2, mais en conservant une résistance suffisante à l'effort tranchant. La section 2 se transforme donc en une rotule (figure 5.b.). L'effondrement du système se produit quand la poutre cède dans la section d'enca斯特rement ;
 - la poutre cède d'abord en 1, qui devient une rotule libre (figure 5.c.). Le système se comporte alors comme une poutre biarticulée jusqu'au moment où il cède en 2, ce qui amène son effondrement.

Dans ce cas, le comportement du système peut être représenté par un modèle parallèle fragile.

c) S'il s'agit d'un matériau possédant une ductilité appréciable (par exemple une poutre en acier), la rupture se produit par formation du mécanisme de ruine de la figure 5.d.

Le modèle de comportement est alors le modèle parallèle ductile.

3.2. En ce qui concerne la relation entre la sécurité d'un élément et la sécurité d'ensemble, la figure 6 permet de comparer le coefficient n' , correspondant au modèle série, avec le coefficient n'' , correspondant au modèle parallèle ductile. Ils ont été définis par l'un des auteurs [6] comme le facteur par lequel il faut multiplier le coefficient de sécurité central d'un élément isolé pour que la probabilité de survie de la structure soit la même que celle de l'élément isolé.

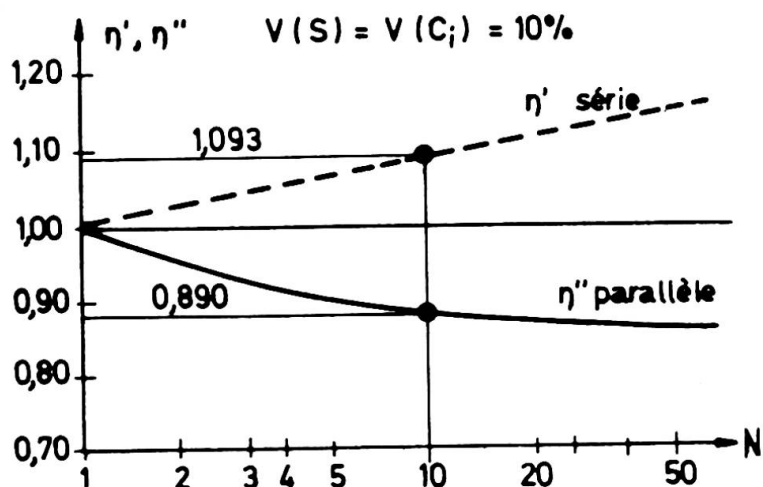


Figure 6

La comparaison est établie pour une probabilité de survie de la structure de $1 - 10^{-3}$ et une même distribution (logarithmo-normale) de l'action et des capacités portantes des éléments.

On considère par exemple le cas d'une association de $N = 10$ éléments identiques dont la capacité portante est caractérisée par un coefficient de variation $V(C_i) = 10\%$, qui doit supporter avec une sécurité de $1 - 10^{-3}$, une action S de coefficient

de variation $V(S) = 10\%$. Si les 10 éléments sont disposés en série, le coefficient n' doit avoir la valeur 1.093. S'ils sont disposés en parallèle, n'' doit valoir 0.890.

Le tableau ci-dessous indique la valeur qu'il faut donner à la probabilité de survie d'un élément pour assurer à l'ensemble des 10 éléments une probabilité de survie de $1 - 10^{-3}$ dans les trois associations envisagées.

| Modèle | série | parallèle fragile | parallèle ductile |
|---------------|---------------|------------------------|-------------------------|
| $P_{(+)}^o i$ | $1 - 10^{-4}$ | $1 - 53 \cdot 10^{-4}$ | $1 - 120 \cdot 10^{-4}$ |

3.3. Pour le modèle série qui schématisé le comportement des constructions dont la ruine d'un élément amène la ruine d'ensemble, nous avons montré [1], [4], [6] que chaque élément doit avoir une probabilité de survie égale à

$\sqrt[N]{P_{(+)}^o}$ ($N =$ nombre d'éléments) pour que la probabilité de survie de la structure soit au moins égale à $P_{(+)}^o$.

Puisque pour n'importe quelle valeur de $N > 2$ l'inégalité

$$\sqrt[N]{P_{(+)}^{\circ}} < \sqrt[N!]{P_{(+)}^{\circ}} \quad (5)$$

est vérifiée, on peut affirmer que :

Pour un même nombre d'éléments, N , et pour une même probabilité de survie du système, $P_{(+)}^{\circ}$, la sécurité d'un élément faisant partie d'un modèle série est toujours inférieure à la sécurité d'un chemin de ruine possible associé à un modèle parallèle fragile.

4. COMPORTEMENT DU TYPE MIXTE.

Beaucoup de structures se caractérisent par un comportement mixte (ductile-fragile) [2]. C'est le cas des constructions dont les sections ne possèdent qu'une capacité limitée de déformation plastique avant la ruine. Dans certaines circonstances, les deux types de comportement peuvent apparaître successivement. Par exemple, si plusieurs éléments mixtes (acier-béton) d'une structure sont soumis à un effort de traction, le béton épouse rapidement sa capacité de résistance en traction et se rompt (comportement fragile). L'effort est alors repris uniquement par l'acier dont le comportement est essentiellement ductile.

Une telle structure peut être schématisée par un modèle mixte présentant des éléments disposés à la fois en série et en parallèle (cfr. figure 4). L'évaluation exacte de la probabilité de survie s'avère, dans ce cas, pratiquement impossible. Néanmoins, on peut établir des bornes d'un intervalle qui encadre la valeur exacte de cette probabilité [4].

5. CONCLUSIONS.

Cette étude complète notre contribution au Rapport Préliminaire [1]. On analyse, du point de vue probabiliste, deux autres types de comportements : parallèle fragile et mixte.

La complexité du problème rend pratiquement impossible l'évaluation exacte de la sécurité, mais de tels modèles fournissent à l'ingénieur des indications précieuses pour l'évaluation de la sécurité des structures par rapport aux différents types de comportements structuraux.

BIBLIOGRAPHIE.

- [1] DOTREPPE, J-C., et FRANGOPOL, D. : Sensitivité de la Sécurité des Constructions par rapport aux Types de Comportements Structuraux. Rapport Préliminaire, 10ème Congrès de l'AIPC., Tokyo, Septembre, 1976, pp.51-56.
- [2] ESTEVA, L. : Lessons from Some Recent Earthquakes in Latin America. Proceedings, 4 th World Conference on Earthquake Engineering, Santiago, Chile, 1969.
- [3] FRANGOPOL, D. : Statistical Properties of the Structural Reliability in the Elastic and Elasto-Plastic Range. Revue Roumaine de Sciences Techniques, Série de Mécanique Appliquée, No.5, Bucarest, 1974, pp. 879-889.

- [⁴] FRANGOPOL, D. : Modèles d'Analyse de la Sécurité et de l'Optimisation des Structures dans un Contexte Probabiliste. Rapport No.49, Service de Mécanique des Matériaux et de Statique des Constructions, Université de Liège, Juin, 1974.
- [⁵] FRANGOPOL, D., et DOTREPPE, J-C. : Considérations sur la Sécurité des Structures par rapport aux Différents Etats Limites de Comportement. Rapport Préliminaire, Colloque Inter-Associations AIPC-FIP-CEB-RILEM-IASS, Liège, Juin, 1975, pp. 501-511.
- [⁶] FRANGOPOL, D. : Etude Probabiliste de la Sécurité des Constructions. Thèse de Doctorat, Université de Liège, 1976.
- [⁷] FRANGOPOL, D. : Structural Systems Reliability Analysis. 2nd International Conference on Applications of Statistics and Probability in Soil and Structural Engineering, Aachen, September, 1975, pp.131-140.
- [⁸] YAO, J.T.P., et YEH H-Y. : Formulation of Structural Reliability. Journ. Struct. Div., Proc. ASCE, Vol. 95, No. ST.12, December, 1969, pp.2611-2619.

RESUME

On examine du point de vue probabiliste deux types de comportements structuraux: le comportement du type parallèle fragile et le comportement du type mixte. On présente une comparaison qualitative et quantitative entre les différents modèles.

ZUSAMMENFASSUNG

Man untersucht durch wahrscheinlichkeitstheoretische Betrachtungen zwei Typen von strukturellem Verhalten : das parallele spröde und das gemischte Verhalten. Ein qualitativer und quantitativer Vergleich der beiden Modelle wird angestellt.

SUMMARY

Two types of structural behaviour are considered from a probabilistic point of view: the parallel brittle and the mixed types of behaviour. Qualitative and quantitative comparisons are made between different models.

Considerations on Optimum Combination of Safety and Economy

Considérations sur le meilleur compromis entre sécurité et économie

Betrachtungen über den besten Kompromiss zwischen Sicherheit und Wirtschaftlichkeit

DAN FRANGOPOL

Assistant

Institute of Civil Engineering
Bucharest, Rumania

JACQUES RONDAL

Assistant

Institute of Civil Engineering
Liège, Belgium

The report [1] has served to emphasize that engineering design requires methods and concepts of probability. The process of selecting the probability of failure of a structure to achieve a stated objective (e.g. make minimum the total expected cost of the structure) is known as probabilistic optimum based-design [7].

The goal of this discussion is to show that a few useful conclusions can be found in the safety-economy optimization process.

In order to evaluate the total expected cost of a structure C_t , the initial cost C_i , the cost of failure C_f and the probability of failure P_f are to be calculated first. Optimum probabilistic design requires the minimization of C_t :

$$C_t = C_i + C_f \cdot P_f \quad (1)$$

The central safety factor of a structure is very nearly a linear function of $\text{colog}_{10} P_f$ [2], [3], [6] :

$$\theta = \alpha_1 \cdot \text{colog}_{10} P_f + \alpha_2, \quad (2)$$

where α_1 is the increment of central safety factor required to reduce P_f by a factor of 10, and α_2 is a positive constant.

On the other hand, the initial cost C_i may be taken as a linear function of θ [2], [5], [8] :

$$C_i = \gamma_1 \cdot \theta + \gamma_2 = \beta_1 \cdot \text{colog}_{10} P_f + \beta_2, \quad (3)$$

where γ_1 , γ_2 , $\beta_2 = \alpha_2 \gamma_1 + \gamma_2$ are constants coefficients and β_1 is the increment of the initial cost required to reduce P_f by a factor of 10.

Since the cost of failure C_f is generally independent of the initial cost,

equating the derivative of the total cost to zero gives the optimum probability of failure

$$P_{f_{op}} = \frac{\beta_1}{C_f \cdot \ln 10} \quad (4)$$

and the optimum expected total cost

$$C_{t_{op}} = \beta_1 \cdot \text{colog}_{10} \frac{\beta_1}{C_f \cdot \ln 10} + \frac{\beta_1}{\ln 10} + \beta_2 \quad (5)$$

Therefore the expression for the excess cost ΔC_t (overdesign or underdesign) is the following :

$$\Delta C_t = C_t - C_{t_{op}} = \beta_1 \left(\log_{10} \frac{P_{f_{op}}}{P_f} + \frac{1}{\ln 10} \frac{P_f - P_{f_{op}}}{P_{f_{op}}} \right). \quad (6)$$

Assuming $P_{f_{op}} = 10^{-4}$, a plot of $\Delta C_t / \beta_1$ as a function of P_f is shown in figure 1.

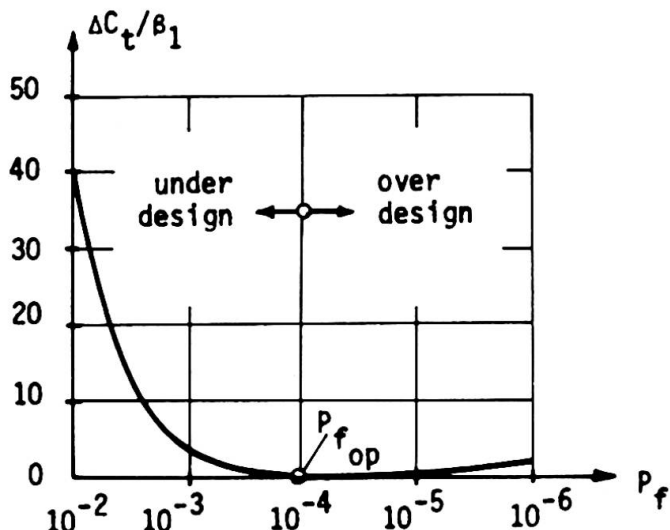


Figure 1 - Excess cost.

It then follows that :

- For the same absolute value of the safety difference

$$D = \text{colog}_{10} P_f - \text{colog}_{10} P_{f_{op}} \quad (7)$$

the underdesign is more expensive than the overdesign ;

- In the region of overdesign, the excess cost is quite insensitive to the P_f variation ;
- In the region of underdesign, the excess cost is very sensitive to the P_f variation.

In the eventuality that damage occurs, the loss C_f (costs of the building, potential loss of human lives and industrial damage caused by the failure) can be expressed as f times the cost C_i [5].

The value of f gives a good indication of the magnitude of the damage that is caused by failure.

The optimum expected total cost (5) is a linear function of $\log_{10} f$ [4] :

$$C_{t_{op}} = \beta_1 \cdot \log_{10} f + a \quad (8)$$

where

$$a = \beta_1 \cdot \text{colog}_{10} C_i \cdot \ln 10 + \frac{\beta_1}{\ln 10} + \beta_2 .$$

A graph of $C_{t_{op}}$ as a function of $\log_{10} f$ is given in Figure 2.

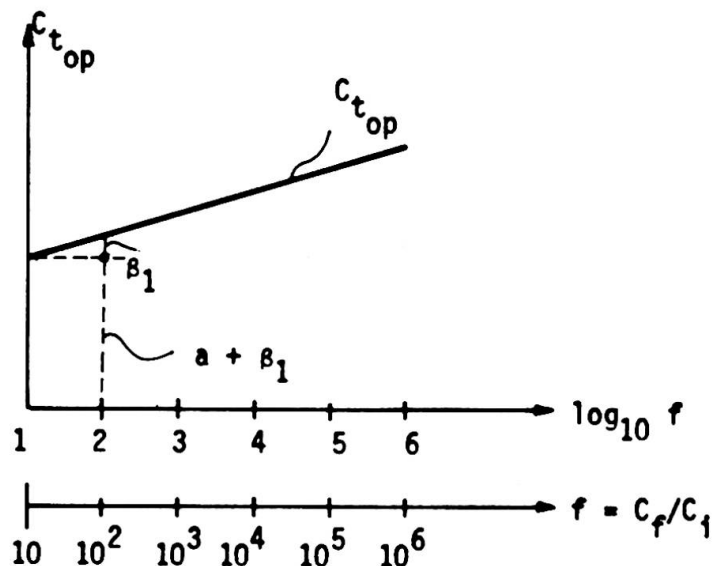


Figure 2 - Sensitivity of the optimal solution.

The foregoing considerations should permit a rational combination of safety and economy, in order to reach a satisfactory approach of an optimum solution.

REFERENCES.

- [1] DICKE, D. : Achievement of Safety and Economy in Design and Construction. Introductory Report, 10th Congress, IABSE, Tokyo, Sept. 1976, pp.17 - 24.
- [2] FRANGOPOL, D. : Discussion sur l'optimisation probabiliste des constructions. La sécurité des constructions. Editions Eyrolles, Paris, 1976. pp. 360 - 362.
- [3] FRANGOPOL, D., RONDAL, J. and NGUYEN, D.H.: Reliability analysis and optimum probability-based design of plastic structures. IUTAM, 14th International Congress, Delft, Sept. 1976.
- [4] FRANGOPOL, D. ; Etude probabiliste de la sécurité des constructions. Doctoral Thesis, University of Liège, 1976.

- |5| LIGTENBERG, F.K. : What safety Margin is necessary in a Structure ? Discussion N° 5, Technical Committee N° 10, ASCE-IABSE International Conference on Planning and design of tall buildings. Vol. DS, Lehigh University, August, 1972, pp. 437 - 442.
- |6| LIND, N.C. and DAVENPORT, A.G. : Towards Practical application of structural reliability theory. Paper SP 31-3, Probabilistic design of reinforced concrete buildings, Detroit 1972, pp. 63 - 110.
- |7| MOSES, F.: Approaches to structural reliability and optimisation. SM Study N° 1, University of Waterloo, Ontario, 1969.
- |8| SANDI, H. : Contributions to the theory of structural design. (Thesis in Roumanian), Institute of civil engineering, Bucharest, 1966.

SUMMARY

Several independent attempts are made to evaluate an optimal value for the probability of failure and for the expected total cost. The sensitivity of the optimal solution to the magnitude of the damage that is caused by failure is also analysed.

RESUME

Plusieurs tentatives indépendantes sont faites pour obtenir la valeur optimale de la probabilité de ruine et du coût total attendu. La sensibilité de la solution optimale par rapport à l'importance du dommage causé par la ruine est également analysée.

ZUSAMMENFASSUNG

Verschiedene unabhängige Untersuchungen werden gemacht, um den optimalen Wert der Versagenswahrscheinlichkeit mit bezug auf die zu erwartenden Totalkosten festzulegen. Die Abhängigkeit der optimalen Lösung von der durch den Bruch verursachten Schadengrösse wird auch analysiert.

Results of the Application of Stochastic Programming for the Computation of Safety of Structures

Résultats de l'application de la programmation stochastique pour le calcul de la sécurité des structures

Ergebnisse aus der Anwendung der stochastischen Programmierung für die Berechnung der Sicherheit von Konstruktionen

O. KLINGMÜLLER
 Dipl. Ing.
 Gesamthochschule Essen
 Essen, BRD

To the proposed application of stochastic programming for the computation of safety I want to make some additional remarks. My first point deals with the comparison of the well-known method of computing the probability of failure of structures on the basis of Failure Modes /1/ with the proposed concept. The second remark concerns the application of the proposed concept to the limit load analysis by nonlinear programming.

1. On the left hand side of figure 1 we have a formulation of the first limit load theorem as a linear programming problem. The solution of this primal problem gives us the maximum of the load factor which holds the equilibrium conditions as well as the linearized yield conditions, both combined in the matrix \underline{B} . In this special formulation the vector of primal variables \underline{y} consists of the load factor y_1 and the redundant forces $y_2 \dots y_{p+1}$; p is the redundancy of the structure.

On the right hand side of figure 1 we have a formulation of

| Primal Problem -First Limit Load Theorem | Dual Problem -Second Limit Load Theorem |
|--|---|
| maximize \underline{y}_1 | minimize $\underline{E}'_o \cdot \underline{z}$ |
| subject to | subject to |
| $\underline{B} \cdot \underline{y} \leq \underline{E}_o$ | $\underline{B}'_1 \cdot \underline{z} \geq 1$ |
| $\underline{y} \geq 0$ | $\underline{B}'_i \cdot \underline{z} = 0, i=2 \dots p+1$ |
| \underline{y} : vector of primal variables | $\underline{z} \geq 0$ |
| y_1 : load factor , $y_2 \dots y_{p+1}$: redundant forces | |
| \underline{z} : vector of dual variables, i.e. strain velocities | |
| \underline{B} : matrix, combining linearized yield conditions and equilibrium conditions | |
| \underline{E}_o : vector of the right hand sides (e.g. fully plastic moments) | |
| $\underline{E}_o \cdot \underline{z}$: work of the internal forces | |

Figure 1: Linear Programming Problems for Limit Load Analysis

the second limit load theorem as a linear programming problem. The solution of this dual problem gives us the minimum of the work of the internal forces, i.e. the scalar product $\underline{F} \cdot \underline{z}$. The work of the external forces, given by $\underline{B}' \underline{z}$ must be not less unity. The equality constraints $\underline{B}' \underline{z}$ are the conditions of kinematic compatibility. B_i are columns of B . Solving this dual problem is equivalent to finding the most critical out of all failure modes.

By the theorem of duality in linear programming we know that the load factor, that is the value of the objective function must be the same for both problems. Computing the probability of failure with the proposed concept then means just to look at the probability of failure by the most critical failure mode. Thus we have a lower bound for the probability of failure /1/. This is the reason why the sensitivity analysis becomes very important.

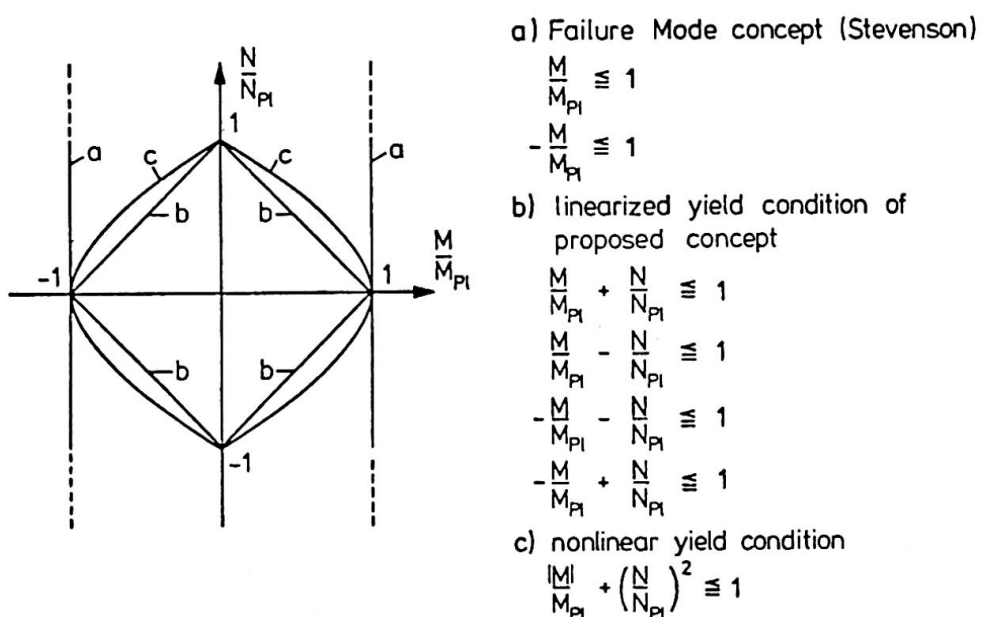
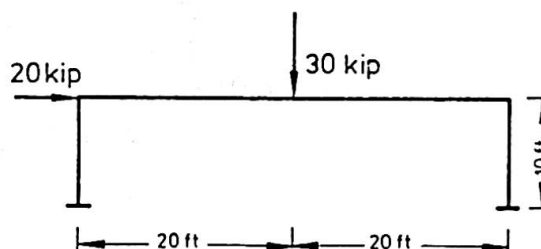


Figure 2 : Yield Conditions of Beam Elements



coefficients of variation: 0.1

| beam | column | Failure Mode concept | | proposed concept | |
|---------------|---------------|----------------------|---------------------|------------------|---------------------|
| mean M_{Pl} | mean M_{Pl} | load factor | p_f | load factor | p_f |
| 200 | 100 | 1.0 | 0.56 | 0.99 | 0.54 |
| 320 | 50 | 1.0 | 0.63 | 0.98 | 0.59 |
| 450 | 75 | 1.5 | $2.1 \cdot 10^{-4}$ | 1.46 | $0.9 \cdot 10^{-4}$ |

Figure 3: Comparison of Different Computation Concepts

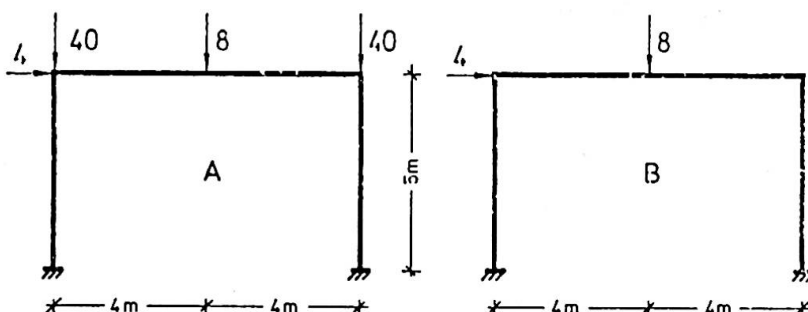
On the other hand in the computing of the probability of failure with regard of all possible failure modes the yield condition "a" in figure 2 is used. An interaction of normal forces and bending moments is either neglected, or the computation demands additional iteration. The lines "b" in figure 2 are bounding the feasible region of the proposed concept. The curves "c" belong to the quadratic function for the interaction of normal forces and bending moments.

For the comparison of the results which are given in figure 3 for Stevensons' test example /1/ we therefore must have in mind different yield conditions and different computation concepts.

2. The difference between the nonlinear yield condition and the linearized yield condition (figure 2) leads to the idea of computing the limit load by means of nonlinear programming. The nonlinear programming problem for limit load analysis is given in figure 4. An iterative method yields a solution of this problem. In the solution a number of yield conditions hold the equality sign. These nonlinear yield conditions are expanded into a Taylor series around the solution and around the stochastic variables F_o . The nonlinear terms are suppressed and this results in a linear transformation of the stochastic variables F_o into the unknowns λ, \underline{x} . With such a linear transformation we can apply the described concept to the limit load analysis by nonlinear programming.

| |
|--|
| $\begin{aligned} & \text{maximize } \lambda \\ & \text{subject to} \\ & \Phi_i(\lambda, \underline{x}, F_{oi}) \geq 0 \quad i = 1 \dots r \\ & \lambda \geq 0 \end{aligned}$ <p>λ : load factor \underline{x} : vector of redundant forces F_{oi} : plastic load bearing capacities (e.g. fully plastic moments) Φ_i : nonlinear yield conditions r : number of control points</p> |
|--|

Figure 4 : Nonlinear Programming Problem for Limit Load Analysis



$$M_{Pl} = 17.4 \text{ [Mpm]}, N_{Pl} = 210.9 \text{ [Mp]} \text{ in all sections}$$

$$\text{coefficients of variation: } c_v^P = 0.2, c_v^{M_p} = 0.1$$

| | system A | | system B | |
|-------------|---------------------|---------------------|---------------------|---------------------|
| | linear | nonlinear | linear | nonlinear |
| load factor | 1.56 | 1.81 | 1.93 | 2.00 |
| P_f | $5.3 \cdot 10^{-3}$ | $6.6 \cdot 10^{-5}$ | $1.9 \cdot 10^{-5}$ | $4.5 \cdot 10^{-6}$ |

Figure 5 : Comparison of Linear and Nonlinear Programming in Limit Load Analysis.

The results of linear and nonlinear programming in limit load analysis are compared in figure 5 with two different loading conditions. The differences in the probability of failure are caused mainly by the different load factors. The greater load factors of the nonlinear solution are due to the larger feasible region of the quadratic yield condition.

The design of structures for a given allowable probability of failure requires a solution of the above described problems in every step of iteration, i.e. computing the load factor and the probability of failure for given cross sections of the elements. For a single structure the computertime for a reliability-based design might cost too much. But if we look at problems like optimizing prefabricated elements for a large number of buildings or like the optimization of a building code for given restricted resources /2/ it is important to find structures with minimum cost which are safe. With the proposed concept I hope to have given a more general way of evaluating the safety of structures with regard to their mechanical properties.

References

- /1/ Stevenson, J.: Reliability Analysis and Optimum Design of Redundant Structural Systems with Application to Rigid Frames. Ph.D. Thesis, Case Western Reserve University 1968
- /2/ Ravindra,M.K. and Lind,N.C. : Theory of Structural Code Optimization. Journal of the Structural Division, ASCE, Vol.99 N° ST 7 , July 1973 , p. 1541-1553

SUMMARY

Results obtained with the proposed concept for the computation of the probability of failure as it was described in the preliminary report are compared to results which are given by the well-known method of computing the probability of failure on the basis of failure modes. A second part of the paper deals with the application of the proposed concept to the limit load analysis by nonlinear programming.

RESUME

Les résultats de l'application de la programmation stochastique pour le calcul de la sécurité des structures - méthode présentée dans le Rapport Préliminaire - sont comparés avec les résultats donnés par le calcul de la probabilité de ruine utilisant la méthode des chaînes cinématiques . La seconde partie de l'exposé montre l'application de la méthode proposée au calcul à l'état limite, utilisant la programmation non-linéaire.

ZUSAMMENFASSUNG

Ergebnisse des im Vorbericht beschriebenen Verfahrens zur Berechnung der Versagenswahrscheinlichkeit von Konstruktionen werden mit der bekannten Methode, die Versagenswahrscheinlichkeit mit Hilfe der kinematischen Ketten zu bestimmen, verglichen. Der zweite Teil des Beitrags behandelt die Anwendung des vorgeschlagenen Verfahrens auf die Traglastberechnung mit nichlinearer Programmierung.

Improved Design Philosophy for the Structural System of Oil Storage Tanks

Un concept pour améliorer la structure porteuse des réservoirs à essence

Über verbesserte Entwurfsgrundlagen für das Tragsystem von Oeltanks

FUKUZO SUTO

Dr. Eng., Chief, Computer Dpt.

HIDEYUKI TADA

Dr. Eng., Senior Struct. Eng.

AKIRA WADA

Struct. Analyst, Computer Dpt.

Nikken Sekkei Ltd./Planners/Architects/Engineers

Tokyo, Japan

1. Introduction

In December 1974, a large oil storage tank in a tank farm located in Western Japan collapsed due to cracks developed at the corner bottom plate. The collapse caused large amount of oil to flood into the sea, thereby giving serious damage to its biological environment. The accident urged re-examination of the safety of similar tanks. Under such circumstances, the authors' firm was asked to study and analyze the structural safety of large cylindrical tanks constructed on a deep reclaimed site in Yokohama City.

The investigation was aimed at: firstly, recommending measures to improve structural safety of tanks on the basis of fundamental considerations on them (Fig. 1) and comprehensive evaluation of the data obtained through the authors' observation of 18 emptied tanks which have sunk at a considerable degree; and secondly, analyzing static and dynamic behaviours of cylindrical oil tank constructed on deep, heterogeneous, loose soil easily subject to consolidation settlement, and establishing certain design criteria to be used as guidelines by the municipal authorities.

The present paper deals with comparative analyses of essential matters involved in "flexible-flexible" structures (Fig. 2) on a basis of the test findings and design improvement proposal derived from a series of analysis.

Fig. 1 Comparison of Present Modelling with Real Structure

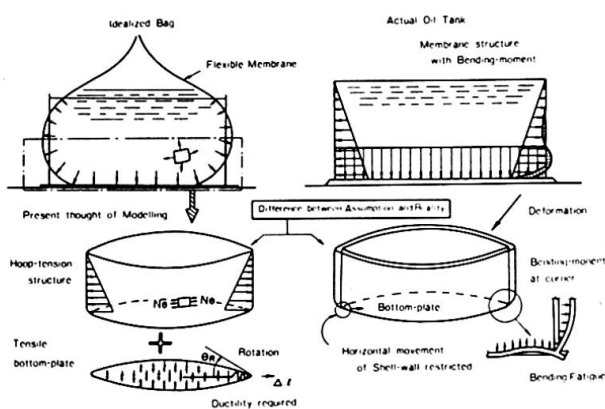
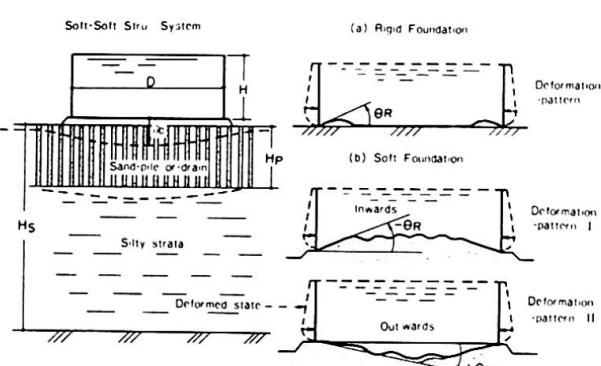


Fig. 2 Structural System and Bottom Plate Deformation Pattern



2. Behaviours of 18 Emptied Tanks

The tested tanks are grouped into three types, namely, 10,000 k ℓ tanks (25 to 42 m diam. and 12 to 21 m high); 30,000 k ℓ tanks (48 to 55 m diam. and 15 m high); and 63,000 k ℓ (64 m diam. and 22 m high).

The tanks are underlain by the loose soil stratum of which volume compressibility coefficients (m_{vC}) range from 0.5 to 2×10^{-2} cm 2 /kg in a depth of 20 to 50 m below grade. The soil is, in a range down to 7 to 23 m, stabilized by sand-drain method using 40 to 50 cm diam. pipes.

As compared with the levels recorded upon the completion of tanks, overall absolute settlements of tanks were 30 to 195 cm at circumferential places of the tank and differential settlements were 10 to 80 cm between the center and the edge. In some instances, mean residual deformation angles, overall settlements and differential settlements were in considerable agreement with those obtained from FEM analyses of a monolithic tank-soil model as shown in Table 1. By this, authors could have the confidence to proceed to detailed theoretical analysis.

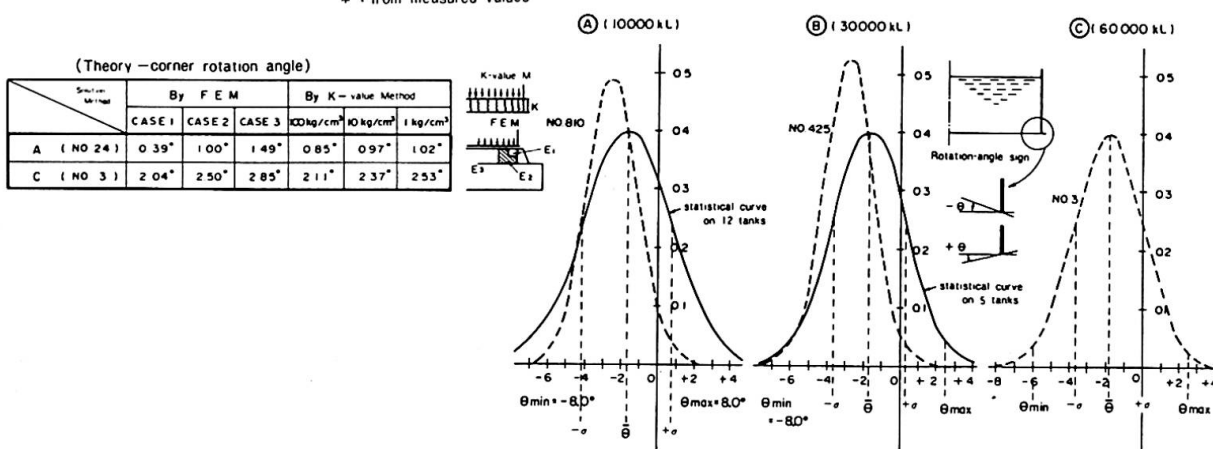
The utmost emphasis in the checking was given to the corner at which shell and bottom plates are joined by fillet welding. As shown with statistical curves in Fig. 3 gained from processing measured data aquired at places of 2 m pitch along circumference of tanks, the plastic residual deformation angles of bottom plates at the corner due to the forced bending moment arising from filled or empty state of tank on plastically deformed supporting soil were found to be about two or three degrees on an average, though each measured value varied depending on the construction conditions. At some points where the underlying soil was very loose, an angle of as much as eight degrees was found.

Table 1 Tank-dimensions Measured and Theoretical values

| | D (m) | H (m) | Clay Depth (m) | Foundation | θ for Circumferential | θ B = + | Number measured |
|-----------------|---------------|---------------|----------------|---------------------------|------------------------------|----------------|-----------------|
| 10,000 k ℓ | 25.00 ~ 42.53 | 12.20 ~ 21.00 | 8 ~ 4.8 | Sand-pile and sand-drain | 65 ~ 140 | -174° | 12 |
| | | | | | | | |
| 30,000 k ℓ | 48.45 ~ 54.26 | 15.28 | 21 ~ 4.6 | Preloading and Sand-drain | 60 ~ 195 | -173° | 5 |
| | | | | | | | |
| C | 63.90 | 21.90 | 40 | Vibro-rotation | 180 | -186° | 1 |

* : from measured values

Fig. 3 Statistical Distribution of Rotated Angle



3. Theoretical Analyses of Tanks Constructed on Loose Soil

The tanks now under consideration are a kind of membrane structures subject to bending constraints at the shell-to-bottom joint. In addition, the tanks stand on loose soil whose properties remain unclarified by a quantitative analysis. Thus, it is theoretically difficult to make an accurate model that can properly represent these structures. For the purpose of present study, however, an attempt was made which could enable FEM-parametric

studies to be applied, regarding the tank and the soil as single structural body. As an important step, equivalent Young's moduli of soil easily subject to consolidation settlement were determined on the basis of a presumption that δ - ϵ curve properties of them could be regarded as a pseudo-elastic body.

By applying FEM to the semi-infinite elastic solid constituted by thick layers of loose soil with circular pressure loaded upon the surface, displacement and pressure distribution in the soil, and particularly the range of concentrated stresses in the soil located directly below the tank shell were obtained. Then, based on the stress-concentrated area thus determined, elasto-plastic transitional range for the tank and soil was established in a number of stages, and a local area at the shell-bottom junction was taken out and given parametric studies to see the behaviours in the plastic range as a single structural body. Thus obtained are parametric changing conditions of bending deformation and stresses in the bottom plate at the junction and in the soil as illustrated in Table 2.

Thereafter, in order to assist in considerations about detail improvements and formulation of practical calculation method, changing conditions of the bending moments and deformation of the junction were ascertained by giving parametric changes to tank-supporting soil spring while making reference to soil's subgrade reaction coefficients as found experimentally in the existing compacted soil foundation as shown in Table 3.

Inferred from these analytical results, three types of hysteresis loop on bending moment to curvature corresponding to the kind of combination of the mechanical state of corner bottom plate with the degree of deformation characteristics of its foundation are thought to exist as illustrated in Fig. 4.

From various considerations on them the type ③ may be said much more better and safer even for bending fatigue in reference to fracture mechanics.

Table 2 Parametric Analysis Results by FEM with Corner Portion
Combination of Young's Modulus of Soil
 unit: kg/cm^2

| | E_1 | E_2 | E_3 |
|--------|-------|-------|-------|
| CASE 1 | 130 | 130 | 130 |
| CASE 2 | 13 | 65 | 130 |
| CASE 3 | 3 | 13 | 65 |

Mechanical State of Corner Bottom Plate

| | σ_b (kg/cm^2) | δ_v (mm) | P_a (kg/cm^2) | θ_R ($^\circ$) |
|--------|------------------------------------|-------------------------------|-------------------------------|----------------------------|
| CASE 1 | 575 (-446) | 960 | 420 | 204 |
| CASE 2 | 214 (-1067) | 115 | 132 | 250 |
| CASE 3 | 100 (-1326) | 146 | 61 | 285 |

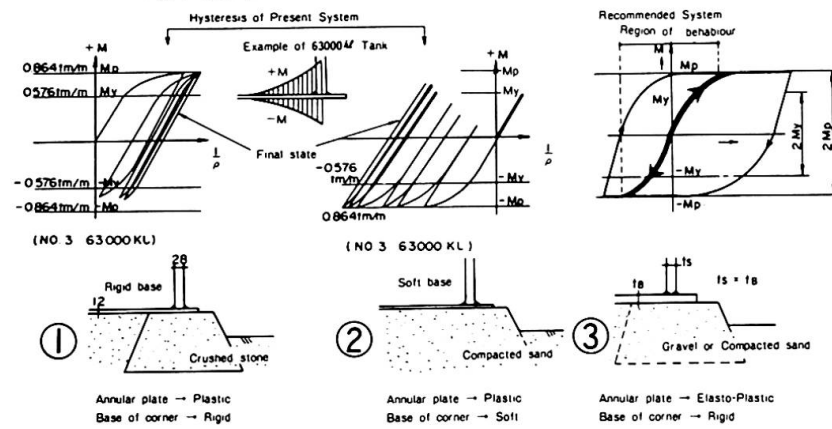
Note:
 $E_1, E_2, \text{ and } E_3$ → in parametric series
 σ_b → Bending stress of bottom plate
 σ_a → (\square) → force stress by on press
 σ_a → (\triangle) → force calculated
 σ_a → (\times) → elastic stress

Table 3 Mechanical State Values on Improved Corner Details

| | $K = 1000 \text{ kg/cm}^2$ | $K = 100 \text{ kg/cm}^2$ | $K = 10 \text{ kg/cm}^2$ | $K = 1 \text{ kg/cm}^2$ |
|-------------|---|---|---|---|
| Improved 1) | δ_v (mm) (0.755) P_a (kg/cm^2) (75.50) M_a (kg/m) (2.06) σ_a (kg/cm^2) (18.66) | 0.435 (1.95) 17.50 (19.50) 3.51 (1.30) 2.74 (5.50) 3.09 (0.80) 2.40 (3.40) 2.28 (2.07) | 1.75 (1.95) 5.70 (15.71) 7.51 (15.71) 4.47 (1.304) | 2.73 (1.304) 2.73 (1.304) 2.93 (0.48) 4.47 (1.304) |
| Present | δ_v (mm) (0.62) P_a (kg/cm^2) (62.40) M_a (kg/m) (3.75) σ_a (kg/cm^2) (2.91) | 2.10 (21.00) 7.51 (7.51) 2.48 (2.48) 1.71 (1.71) | 5.70 (15.71) 7.51 (15.71) 2.62 (2.62) 1.82 (1.82) | 2.73 (1.304) 4.47 (1.304) 1.82 (1.304) |
| Improved 2) | δ_v (mm) (0.62) P_a (kg/cm^2) (62.40) M_a (kg/m) (3.75) σ_a (kg/cm^2) (2.91) | 2.10 (21.00) 7.51 (7.51) 2.48 (2.48) 1.71 (1.71) | 5.70 (15.71) 7.51 (15.71) 2.62 (2.62) 1.82 (1.82) | 2.73 (1.304) 4.47 (1.304) 1.82 (1.304) |

TANK SCALE 63,000 KL D = 63.90m H = 21.90m

Fig. 4 Moment-Curvature Curves for Corner Bottom Plate



In order to see dynamic behaviours of the assumed tank-soil structure during earthquakes, response analyses of liquid contained in a rigid cylinder were made using ground surface waves in which long natural components are predominant as measured for reclaimed loose land and a few kinds of other ordinary strong waves. Fig. 5(a) shows a typical liquid response to the Niigata Earthquake-wave in 1964 which has the characteristic of transfer to long period of wave from usual earthquake pattern after occurrence of soil liquefaction, representing the overflow type due to large liquid-surface displacement with the value of 1.7 m shown by sign (D). Fig. 5(b) shows a typical response to the severe Kanto Earthquake-wave on Sept. 1, 1923 restored by Prof. N. Nasu which has the maximum acceleration of 390 gals in the usual strong earthquake pattern, making characteristic of occurrence of very high pressure to shell-wall and bottom plate with the value of 0.8 Kg/cm² shown by sign (P) which forms an important condition for check against the fracture of corner bottom plate at any strong earthquake. With these response analyses the conditions of liquid agitation, the acting pressure distribution on tanks and the deformation of liquid were obtained.

Taking into considerations of the above sloshing effects and using the distribution pattern of active pressure calculated by the seismic coefficient of 0.3 prescribed simply in Japan, asymmetrical aspects of horizontal force acting on the assumed tank-soil structure were elucidated by FEM. From these results, it was found that compressive force, bending moment and special deformation at the tank lower end would possibly cause buckling of the shell plate as shown in Fig. 6.

On the other hand, basic dynamic analyses by both frequency-analysis-method and earthquake response of tanks were conducted on the rocking and sway motions, regarding the tank as a rigid body supported by vertical and horizontal springs, and sinking of the shell into the foundation in various cases was measured as shown in Fig. 7. The results calculated on the

Fig. 5(a) Sloshing Response of 63000k^t Tank (1)

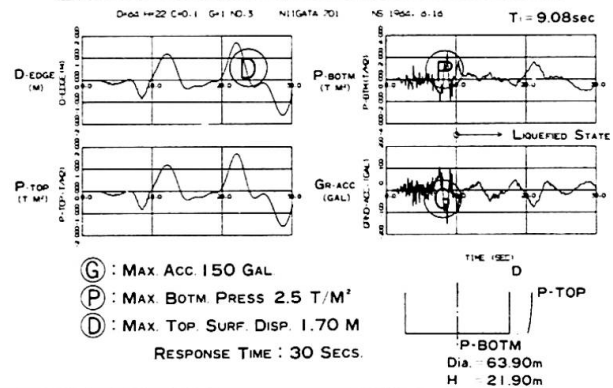


Fig. 5(b) Sloshing Response of 63000k^t Tank (2)

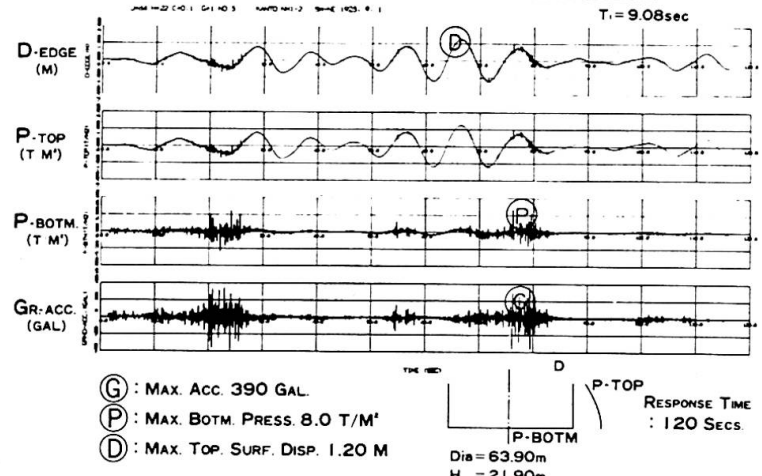
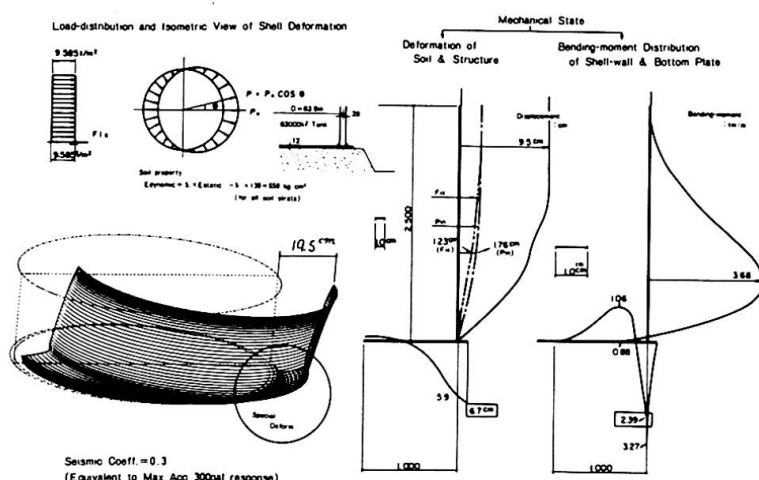


Fig. 6 FEM Analysis on Shell-Soil Str. System for Horizontal Pressure



level of response to earthquake acceleration of 300 gals show that such sinking generally resembles one caused by asymmetrical horizontal force; therefore, large sinking thus caused was considered to lead to large deformation and in some worse cases failure or fracture of the bottom plate.

4. Improvement in Design

From the foregoing analyses, the following were considered a prime consideration in improving the structural safety of large oil tanks constructed on reclaimed land consisting of deep, loose soil in view of preventing dreadful pollution or danger inevitably accompanying huge compensation.

- (1) Compaction methods for loose silt layers should be improved to ensure more effective and economical compaction than is now available. In design practice, the initial consolidation settlement should be standardized and compiled with at higher values than are now commonly adopted as shown in Fig. 8.
- (2) As for the foundation, appropriate detail design should be adopted that will gradually change and decrease, in a number of stages, the equivalent Young's modulus especially for a certain depth and width of foundation located directly below the shell as illustrated in Fig. 9 and 10.
- (3) In combination with such foundation detail, appropriate detail design in shape and weld should be adopted that will ensure the mechanical safety of shell-to-bottom junction against repetitive stresses and fatigue failure as illustrated in Fig. 9 and 10.
- (4) To prevent earthquake damage, appropriate countermeasures should be devised against the liquefaction failure of the ground and the failure of parts of foundation on which the shell-bottom junction is located as illustrated in Fig. 9 and 10.

Fig. 7 Diagram of Vertical Displacement of Corner Portion at Earthquake State

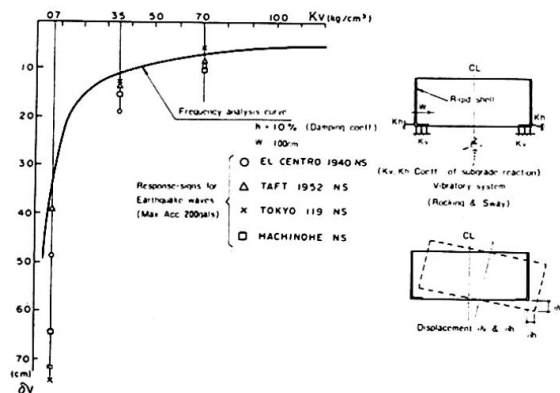


Fig. 8 Recommended Degree of Preliminary Consolidation

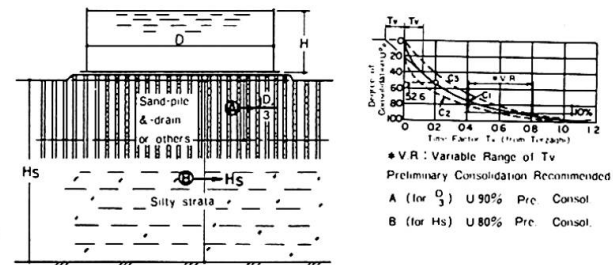


Fig. 9 Example of Improved Detail (1) around the Corner Portion

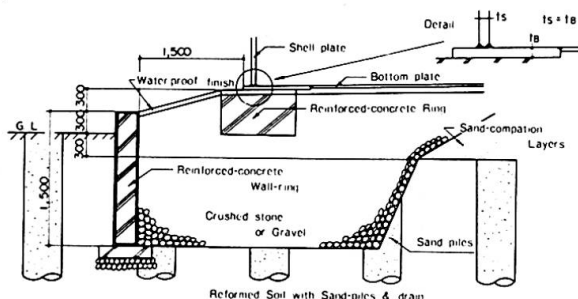
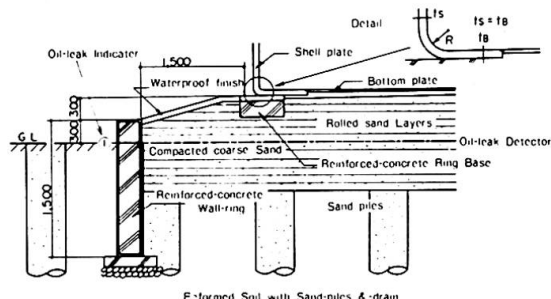


Fig. 10 Example of Improved Detail (2) around the Corner Portion



References

- 1) H. TADA and F. SUTO, "Study on Cylindrical Petroleum Tank-No.1Investigation about the Status quo of Tank-structure and its Peoblematic Points", paper to Gen. Conf. of Architectural Institute of Japan, Autumn, 1975.
- 2) F. SUTO, H. TADA and A. WADA, "Study on Cylindrical Petroleum Tank-No.2 Analysis of Tank-soil Structural System at Filled State of Tank", paper to Gen. Conf. of A.I.J., Autumn, 1975.
- 3) A. WADA, H. TADA and F. SUTO, "Study on Cylindrical Petroleum Tank-No.3 Static Analysis of Tank-shell under Horizontal Force of Sloshing", paper to Gen. Conf. of A.I.J., Autumn, 1975.
- 4) Y. SAITO, H. TADA and F. SUTO, "Study on Cylindrical Petroleum Tank-No.4 Analysis of Rocking and Swaying on Tank when regarded as Rigid Body", paper to Gen. Conf. of A.I.J., Autumn, 1975.
- 5) Reports to Yokohama Municipal Authorities from NIKKEN SEKKEI Task Team, "Reports to Yokohama Investigatory Project on Tank-safety, No.1 ~ No.22", written out from Jan. to Dec., 1975.
- 6) K. TERZAGHI, "THEORETICAL SOIL MECHANICS", JOHN WILLEY AND SONS.
- 7) O. C. Zienkiewicz and Y. K. Cheung, "THE FINITE ELEMENT METHOD IN STRUCTURAL AND CONTINUUM MECHANICS" McGraw-Hill Pub. Comp. Ltd.

SUMMARY

A large tank built on a deep and clayish soil should be a complete flexible-flexible structural system of a pure membrane structure and a soft soil. However, the tank designed by the current standards has unavoidable bending constraints at its corners. The authors have investigated eighteen large tanks, and have compared these with static and dynamic analyses of their flexible-flexible structural system. They propose a concept for improving the design of the tank-soil structural system.

RESUME

Un grand réservoir bâti sur un terrain argileux devrait être un système structural flexible composé d'une membrane et d'une terre molle. Cependant, les réservoirs construits selon les normes courantes présentent inévitablement des contraintes de flexion aux coins. Les auteurs ont fait des mesures sur dix-huit grands réservoirs et ont comparé celles-ci avec les calculs statiques et dynamiques de leur système structural flexible. Ils proposent un concept pour améliorer le projet du système structural réservoir-terre.

ZUSAMMENFASSUNG

Ein auf Tonboden gebauter Oeltank sollte ein flexibles Tragsystem aus einer Membrane und einem weichen Boden darstellen. Der nach den gewöhnlichen Normen gebaute Tank wird aber unvermeidlich Biegespannungen in den Ecken aufweisen. Von den Verfassern wurde die Nachprüfung von achtzehn Behältern durchgeführt, und mit statischen als auch dynamischen, numerischen Untersuchungen verglichen. Verbesserte Entwurfsgrundlagen werden für das Tragwerksystem Tank-Boden vorgeschlagen.

Die Ermittlung der mittragenden Breite im Stützenbereich von Durchlaufträgern

Determination of the Effective Width of Continuous Girders in the Column Zone

Détermination de la bande porteuse des poutres continues dans la région des appuis

W. HOYER F. KERBACH
 o. Professor, Dipl.-Ing. Dr.-Ing.
 Technische Universität Dresden
 Dresden, DDR

Zur Ermittlung des Spannungszustandes von Biegeträgern mit breiten Gurtungen bedient man sich häufig einer mittragenden Breite, um nach den üblichen Methoden der Festigkeitslehre rechnen zu können.

Diese mittragende, ideelle Breite berücksichtigt die Schubverformungen des als Scheibe zu betrachtenden Gurtes und den dabei auftretenden Gurtspannungsverlauf innerhalb des untersuchten Querschnittes.

Zur Bestimmung der mittragenden Breite gibt es eine Reihe bekannter Verfahren, die alle die Darstellung der Momentenzustandslinie als Fourierreihe für die Bestimmung der Scheibenspannungen im Gurt zur Grundlage haben.

Für die Belastung eines Einfeldträgers durch eine konstante Streckenlast oder eine mittige Einzellast und den daraus resultierenden parabolischen bzw. dreieckigen Momentenverlauf lässt sich die mittragende Breite z. B. für den Ort des maximalen Moments ermitteln und für die praktische Handhabung als Kurve über dem Verhältnis Gurtbreite zu Spannweite auftragen (Bild 1). Dabei zeigt sich, daß die Konvergenz der Fourierreiendwicklung beim dreieckigen Momentenverlauf (Bild 1b) wesentlich schlechter ist als beim parabolischen (Bild 1a).

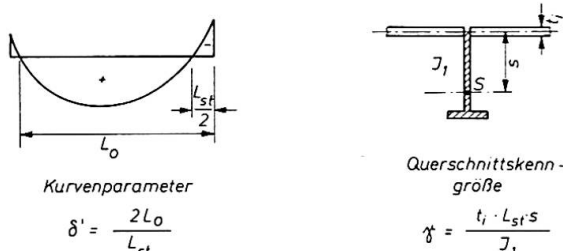
Die Ermittlung der mittragenden Breite gestaltet sich jedoch für den Stützenbereich von Durchlaufträgern weitaus schwieriger, weil der Momentenverlauf sehr unterschiedlich sein kann und die Konvergenz noch schlechter ist. Im Bereich des Stützenmomentes kann die Momentenfunktion allgemein durch

$$M(x) = Ax + Bx^2 \quad (0 = x = L_{st}/2)$$

ausgedrückt werden. Dabei liegt der Momentenverlauf beliebig zwischen den Randwerten $B=0$ (dreieckiger Verlauf) und $A=0, B=q/2$ (Hohlpalabel, Kragarm durch Streckenlast belastet).

Somit wird die Darstellung der mittragenden Breite als Kurve über dem Verhältnis Gurtbreite zu Spannweite praktisch nicht möglich.

Üblicherweise wurde deshalb der negative Momentenbereich von Durchlaufträgern als Dreieck mit gleichem Maximalwert idealisiert und dafür die mittragende Breite berechnet. Als Länge L_{st} dieser Momentenlinie wurde dabei der Abstand der Momentennullpunkte verwendet (Bild 2).



Aus Gründen der Sicherheit einerseits und der Wirtschaftlichkeit andererseits ist es notwendig, ein möglichst genaues Verfahren zu verwenden und gleichzeitig den Momentenverlauf möglichst exakt zu beschreiben.

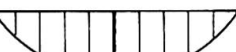
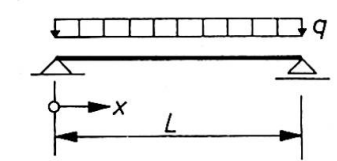
Kehren wir zum betrachteten Stützenbereich zurück, so führt die Erfassung des tatsächlichen Momentenverlaufes gegenüber dem dreieckigen zu einer kleineren mittragenden Breite. Demnach ist aus Gründen der Sicherheit die übliche Idealisierung nicht zu empfehlen.

Die Vergleichsrechnung eines Straßenbrückenhauptträgers über drei Felder mit je 22,5 m Spannweite hat ergeben, daß sich bei Berücksichtigung einer dreieckigen Momentenlinie die mittragende Breite über einer Innenstütze gegenüber dem genauen Wert um 22% zu groß ergibt! Bei unendlich breiten Gurten wäre der Wert sogar um 33% größer!

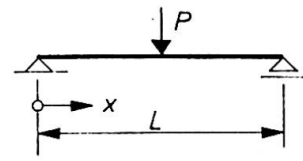
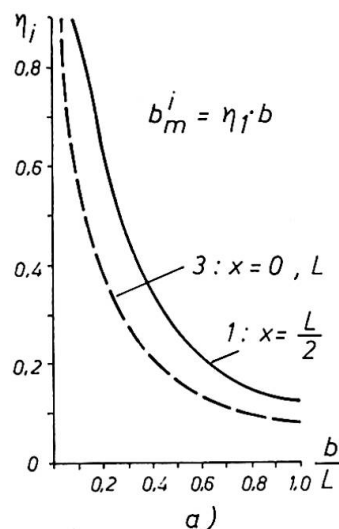
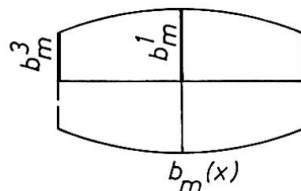
Am Wissenschaftsgebiet Metallbau der Technischen Universität Dresden wurden in Vorbereitung der Überarbeitung unserer Stahlbrückenbauvorschriften Untersuchungen angestellt, um ein einfaches, rasch handhabbares Verfahren zur exakteren Bestimmung der mittragenden Breite zu erhalten.

Als mögliche Lösung wird nun vorgeschlagen, die Länge des Stützmomentenbereiches L_{st} mittels eines Korrekturfaktors α derart zu verkürzen, daß eine dreieckige Momentenlinie der Länge $L' = \alpha \cdot L_{st}$ die genaue mittragende Breite liefert.

Ausgehend von der Charakteristik des Momentenverlaufes $\delta = 2 L_0 / L_{st}$ und einer Querschnittskennzahl des den Gurt unterstützenden Steges γ (Bild 2) läßt sich der Faktor α angeben. Für $\delta = \infty$ erhält man einen geradlinigen Stützmomentenverlauf (also ein Dreieck), damit wird $\alpha = 1,0$. Für $\delta = 1$ ergibt sich die Momentenlinie eines durch eine Streckenlast beanspruchten Kragarmes und α wird zu einem Minimum. In Bild 3 sind die α -Werte für alle denkbaren Stützmomentenverläufe aufgetragen. Dabei liegt α zwischen 0,58 und 1,0. Die gezeigte Kurventafel gilt exakt nur für einen unendlich breiten Gurt.



$$M(x) = \frac{q}{2} x(L-x)$$



$$M(x) = \frac{P}{2} x \text{ für } 0 \leq x \leq \frac{L}{2}$$

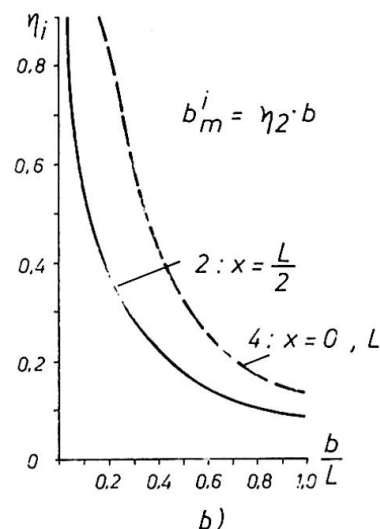
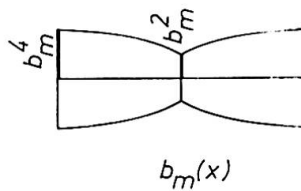


Bild 1 : Mittragende Breite

- a) bei Streckenlastbeanspruchung
- b) bei Einzellastbeanspruchung

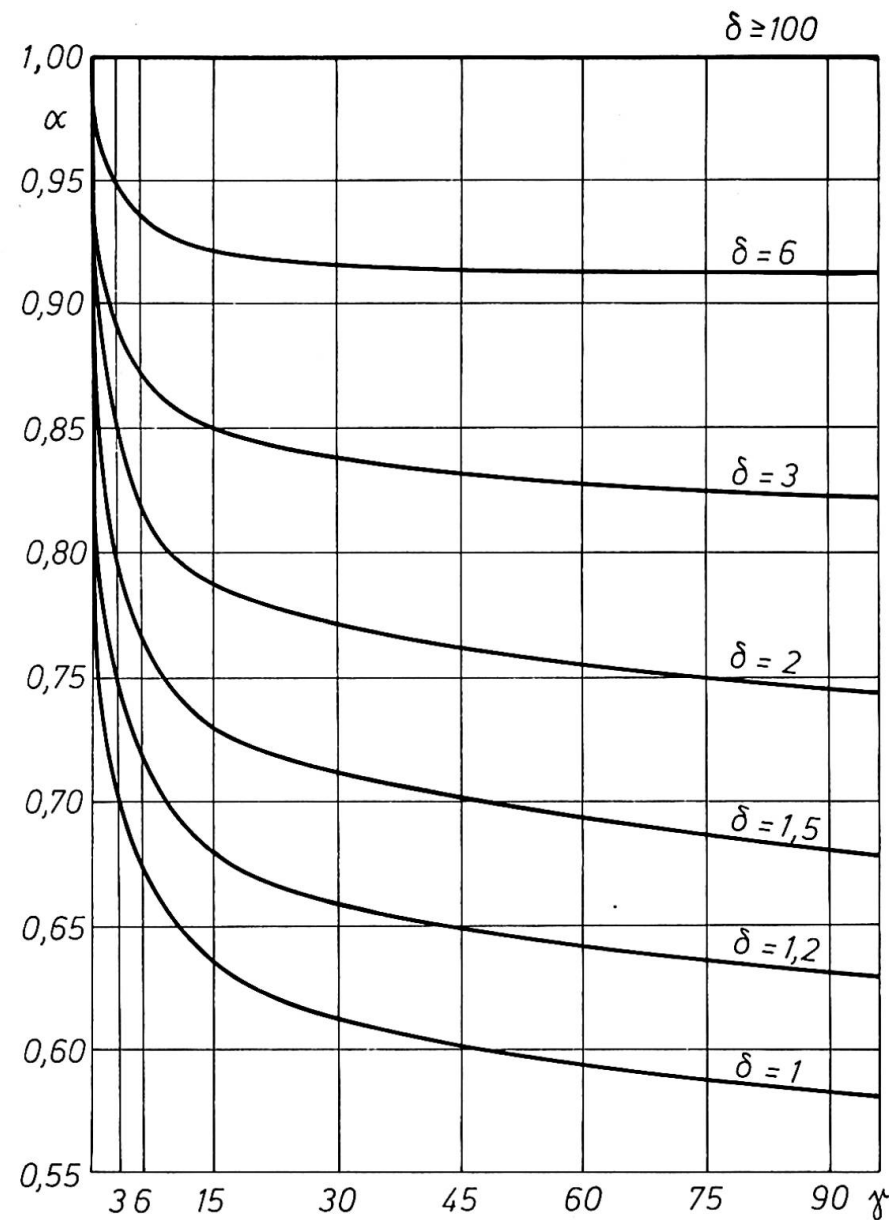


Bild 3 : Korrekturfaktoren α

Wendet man die Korrekturwerte auf die praktisch vorkommenden endlich breiten Gurte an, so erhält man mittragende Breiten, die kleiner sind als die tatsächlichen exakten Werte. Das Verfahren liefert also dann auf der sicheren Seite liegende Näherungswerte, deren Abweichung vom Sollwert geringer ist als bei der Dreieckmethode.

Für das oben zitierte Beispiel beträgt die Abweichung rund 10%.

Es laufen weitere Arbeiten, in deren Ergebnis exakte Werte für andere Randbedingungen der Gurte erhalten werden sollen.

Über die Kenntnis des Korrekturfaktors α läßt sich nun sehr rasch die exakte mittragende Breite bei Benutzung der Werte für eine dreieckige Momentenlinie ermitteln.

Die gezeigte Vorgehensweise gestattet damit eine genauere Erfassung der Tragsicherheit im Stützenbereich, ohne daß der Projektierungsaufwand spürbar erhöht wird.

ZUSAMMENFASSUNG

Zur Bestimmung der mittragenden Breite im Stützenbereich von Durchlaufträgern geht man meist von einer dreieckförmigen Idealisierung der Momentenlinie aus. Dadurch werden auf der unsicheren Seite liegende Ergebnisse erhalten. Der Beitrag zeigt eine Möglichkeit, über eine korrigierte Länge dieser dreieckigen Momentenlinie genauere und sicherere Werte ohne einen spürbaren Berechnungsmehraufwand zu erhalten.

SUMMARY

For determining the effective width of continuous girders in the column zone, mostly one starts from a triangular idealization of the moment curve. The values obtained are consequently on the uncertain side. This contribution shows one way for obtaining more precise and safe values by means of a corrected length of this triangular moment curve without any increase in the calculation.

RESUME

Pour déterminer la bande porteuse de poutres continues dans la région des appuis, on part le plus souvent d'une idéalisation triangulaire de la ligne des moments. On obtient ainsi des résultats se trouvant du côté incertain. L'article montre une possibilité d'arriver à des valeurs plus précises et plus sûres en partant d'une longueur corrigée de cette ligne des moments "triangulaire" sans une augmentation sensible des calculs.

Model Contribution to the Design and Safety Control of Large Structures

Contribution des modèles physiques au projet et au contrôle de la sécurité des grandes structures

Beitrag des Modellversuchs an den Entwurf und die Sicherheitskontrolle von grossen Bauwerken

GUIDO OBERTI

Prof. Ing., President ISMES

Istituto Sperimentale Modelli e Strutture

Bergamo, Italy

1. SAFETY ANALYSIS (ON A MODEL) AND OPTIMIZATION

The model study can be conducted as:

- I) a modern method of stress analysis;
- II) a tool evaluating the critical, or ultimate load.

In case I) the model, usually associated with an electronic processing device, operates as a clever stress calculating machine, and the results obtained can be compared with those provided by using computers of great capacity.

In case II) the ultimate carrying capacity of the structure can be evaluated and the investigation can also concern various types of loads. In this case, the study is completed by determining the "minimum" overall factor of safety of the structure.

2. ELASTIC MODELS

Widely used in stress analysis, they can be subdivided in two groups:

- the first group concerns models of plane structures; the importance of these methods has decreased owing to the ever greater use of the "finite element method".
- The second group generally deals with three-dimensional structures.

In statical tests, electrical deflectometers and extensometers, usually applied to the surface of the model in various directions, measure displacements and strains respectively (fig. 1). The model material may differ from the prototype material, providing it obeys Hooke's law and its Poisson's ratio differs slightly.

The model operates as an "analogical computer", and the final results obtained, easily collected by means of a computer, can be compared with the theoretical ones.

In dynamic tests electromagnetic excitors are applied and piezoelectric accelerometers are used as measuring instruments. The strains are still furnished by strain gauges connected to regular amplifying and recording electrical equipment.

Auxiliary masses are conveniently distributed throughout the model to comply with dynamic similitude (fig. 2).

3. STRUCTURAL MODELS

These serve for testing beyond the elastic range and are usually made of the same materials as the prototype. This is possible for steel and reinforced or prestressed concrete structures when suitable scale (1:5 - 1:20) models are used (fig. 3). But for large structures, such as dams, reasons of economy make it necessary to adopt small scale models (1:50 - 1:150), and then model materials whose mechanical properties are "reduced" with respect to those of concrete, in accordance with similitude.

For these models, ISMES has long been using microconcrete simulating the properties of concrete up to failure, and adopting the technique of "wet" models (with waterproof coating) that are practically without internal stresses.

The tests are conducted in two successive stages. In the first stage, "at working load", the model strains are investigated, under loadings corresponding to the actual working loads.

The second stage concerns "ultimate load tests", and it is made by gradually increasing the applied loads. The ratio between the maximum load actually supported before the collapse and the normal working one is assumed as the overall "factor of safety" of the structure with respect to that "type" of load.

Special mention should be made of earthquake simulation in dynamic tests. ISMES has long had the necessary equipment, which also fully meets all the requirements (fig. 4).

4. GEOMECHANICAL MODELS

These are a speciality of ISMES and investigate structures resting on foundation whose equilibrium or settlement conditions may affect the safety of the structures themselves (large bridges, dams, power or highway tunnels, etc).

5. ON STRUCTURAL SAFETY IN THE DESIGN STAGE

Models are of great importance during the design of large structures, especially if they are structurally complicated and highly hyperstatic.

Of the many cases studied at ISMES, mention is made for:

- the tests carried out on elastic models of large viaducts such as, for instance, the Polcevera and Maracaibo bridge type; or of tall buildings, such as the reinforced concrete building in Montreal, Canada (fig. 5);
- the analysis, by means of structural models carried to failure, of new types of structures. Of the unusual cases mention will be made of the models of prestressed concrete vessels for nuclear reactors and of those of St. Mary's Cathedral in San Francisco, California (fig. 6);

the geomechanical models used to analyze several concrete dams modeled with their foundation, e.g. the Kurobe IV dam (in Japan) and to investigate the stability of power or highway tunnels.

7. ON THE SAFETY FACTOR OF EXISTING STRUCTURES

Models can be of great value when the stability and safety degree of existing structures are to be checked. Particularly when large structures are to be verified, especially when actual statical or dynamic (seismic) conditions were not entirely foreseen in the design stage.

Among the models which yielded highly significant results for evaluating the safety factors brief mention will be made of:

- the failure tests on 1:4 scale models (fig. 7) to investigate the safety of the main columns carrying the "Duomo", i.e. the Cathedral in Milan. The two different materials used (Candoglia marble and Serizzo granite) and the geometry of the individual blocks were identical with those of the prototype.
The stress conditions in the masonry dome bearing the main spire of the Cathedral were also examined on a large 1:15 scale elastic model (fig. 8).
- Sub-horizontal microcracks were found on the upstream of a large Italian arch-gravity dam. The influence of these cracks on the safety was investigated on a large structural model in which the microcracks had faithfully been reproduced.
- The effect of the foundation rock anisotropy horizontally stratified on a gravity dam in Spain was studied on geomechanical models (fig. 9).

REFERENCES: For more details on testing and results, please ask for Technical Bulletins of ISMES - P.O. Box 208, 24100 Bergamo (Italy).

SUMMARY

The present-day contribution of physical models to the design and safety control of large structures are presented; such investigations are systematically carried out at the author's laboratories.

RESUME

La contribution actuelle des modèles physiques au projet et au contrôle de la sécurité des grandes structures est présentée; de telles recherches sont effectuées de façon systématique aux laboratoires de l'auteur.

ZUSAMMENFASSUNG

Der heutige Beitrag des Modellversuchs an den Entwurf und an die Sicherheitskontrolle von grösseren Tragwerken wird dargestellt. Solche Untersuchungen werden systematisch in der Versuchsanstalt des Autors durchgeführt.

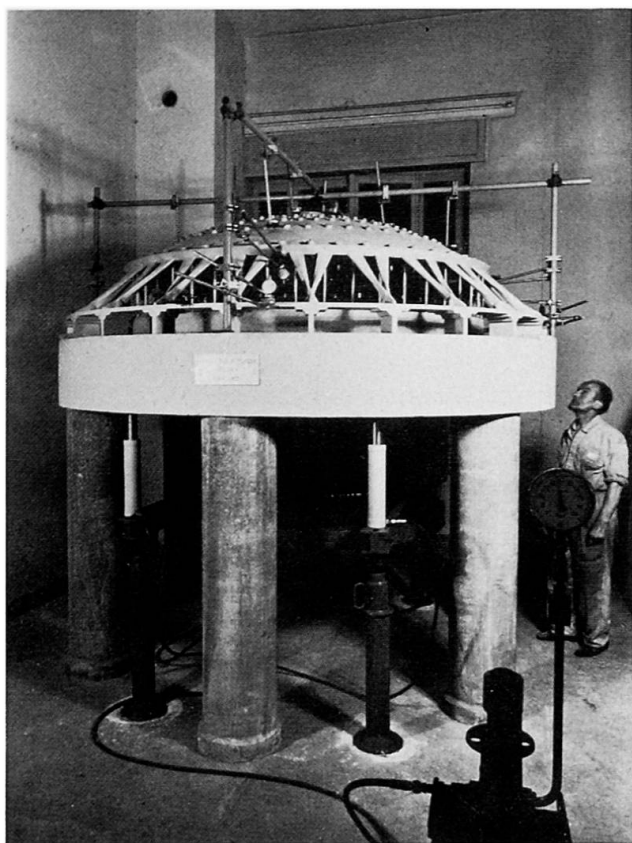


FIG. 1 1:50 scale elastic model of the 130 m dia. circular reinforced concrete shell roof of Norfolk Cultural Center (Virginia, USA). Statical tests.

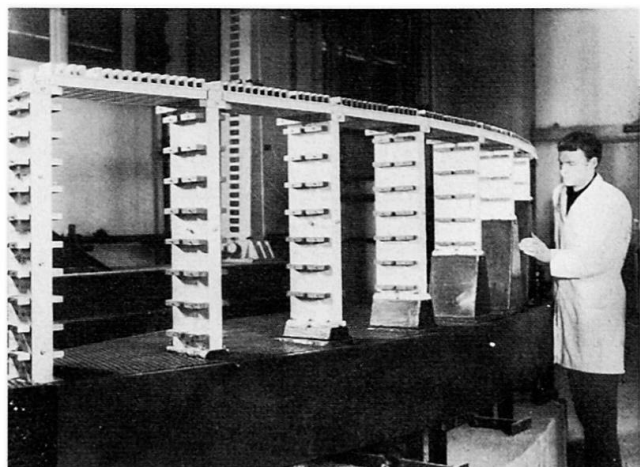


FIG. 2 1:100 scale elastic model of the curved highway viaduct across the Lao river (Calabria, Italy). Maximum height of viaduct piers 80 m. Dynamic tests.

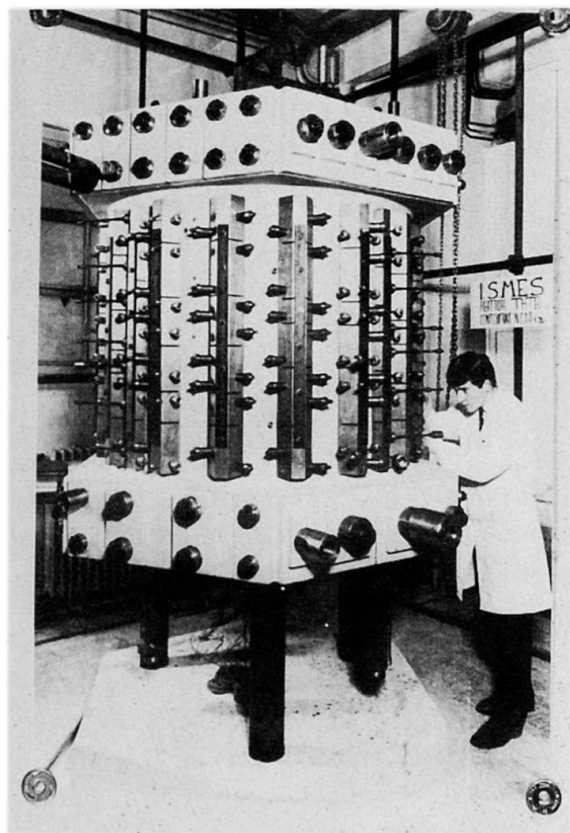


FIG. 3 1:20 scale structural model of the prestressed concrete vessel of the THTR nuclear reactor.

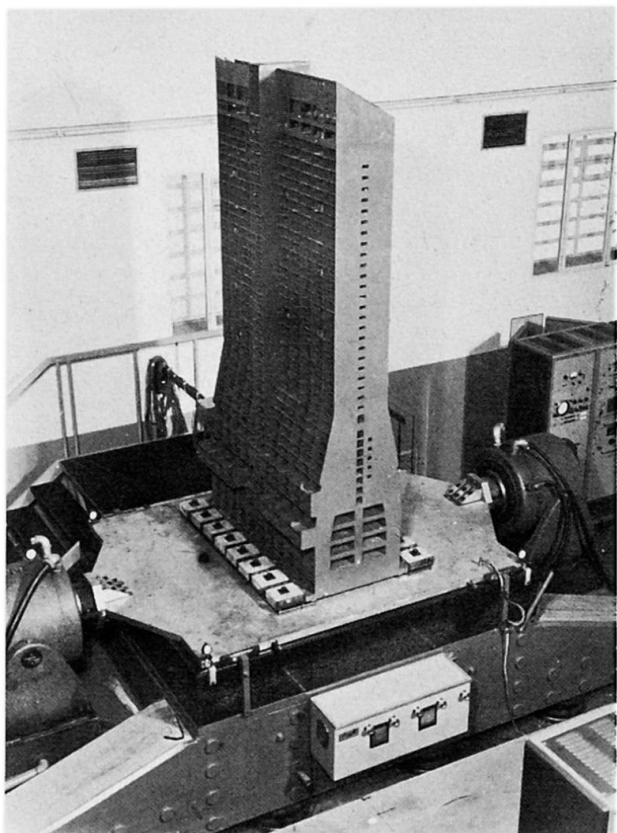


FIG. 4 1:40 scale elastic resin model of Parque Central Skyscraper, Caracas. Dynamic tests taking into account the foundation soil-structure interaction.

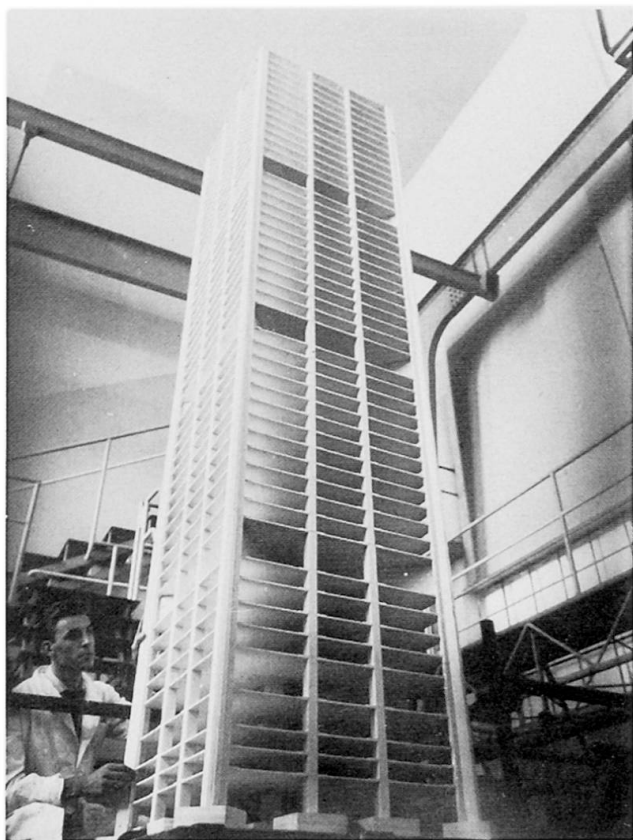


FIG. 5 1:52 scale celluloid elastic model of the 145 m high reinforced concrete building of Place Victoria in Montreal, Canada. Dynamic (seismic) tests.

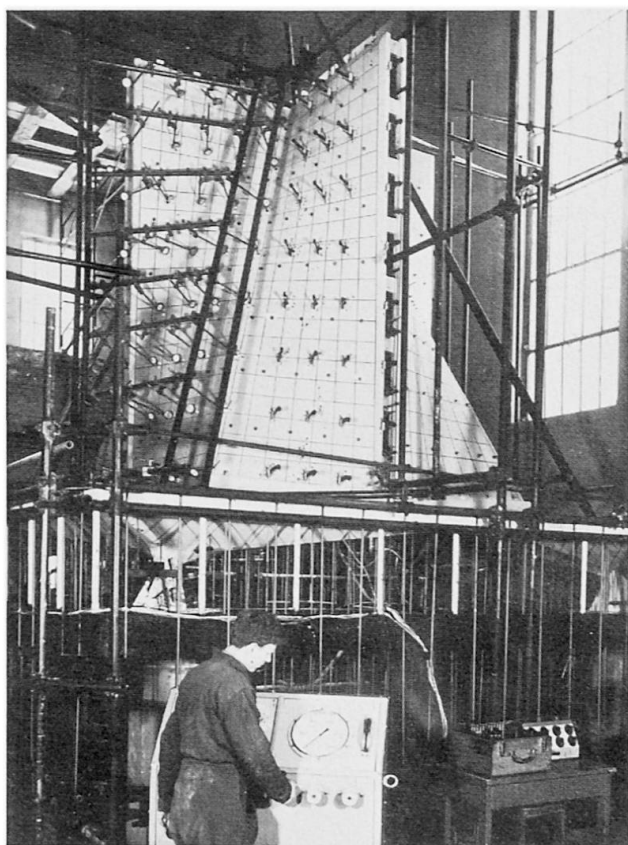


FIG. 6 1:15 scale structural model of the new Cathedral in San Francisco, California, USA, designed by P. L. Nervi. The model is ready for tests to failure.

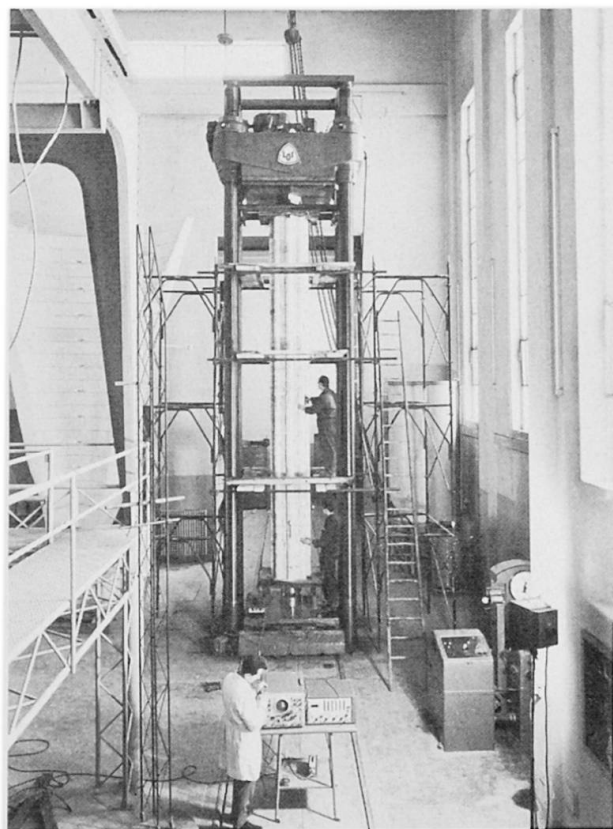


FIG. 7 1:4,7 scale structural model of the main columns carrying the masonry dome of the Cathedral in Milan. The model is ready for the axial compression test.

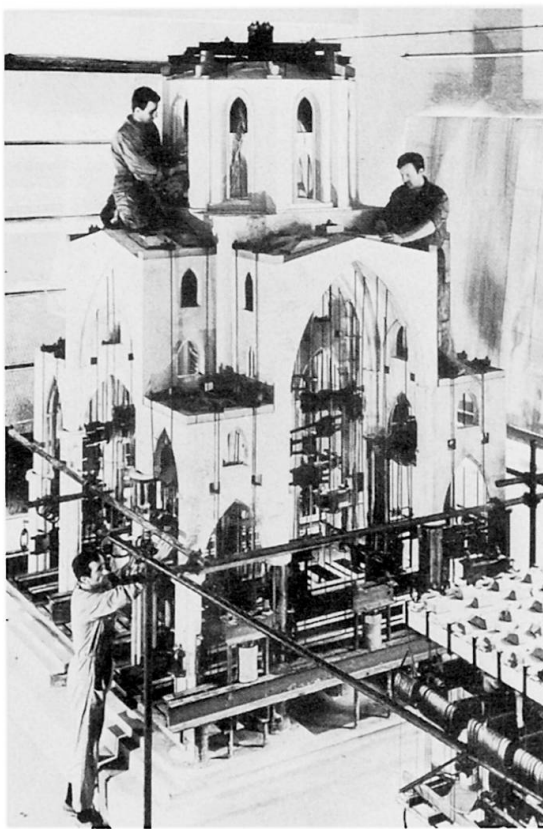


FIG. 8 1:15 scale elastic model of the masonry dome and columns bearing the main spire of the Cathedral in Milan.

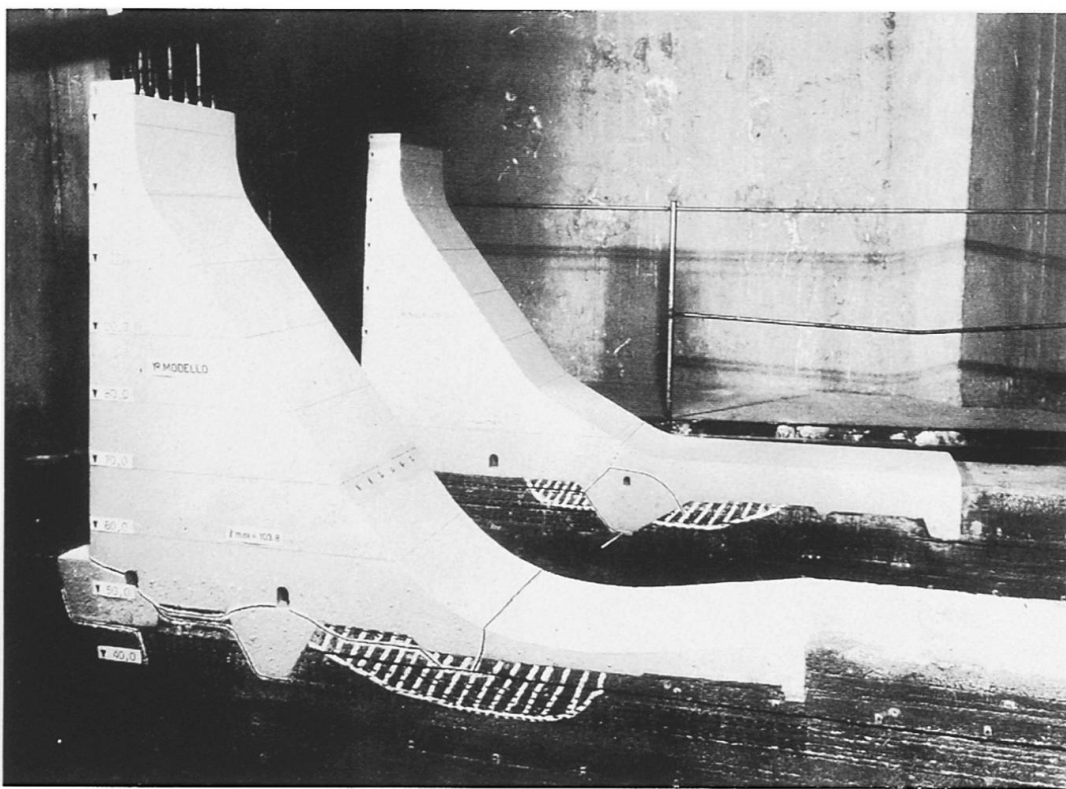


FIG. 9 1:60 scale geomechanical models of a gravity dam in Spain resting on a stratified orthotropic foundation. The tests investigated the effects of the artifices devised to raise the stability of the dam against sliding.

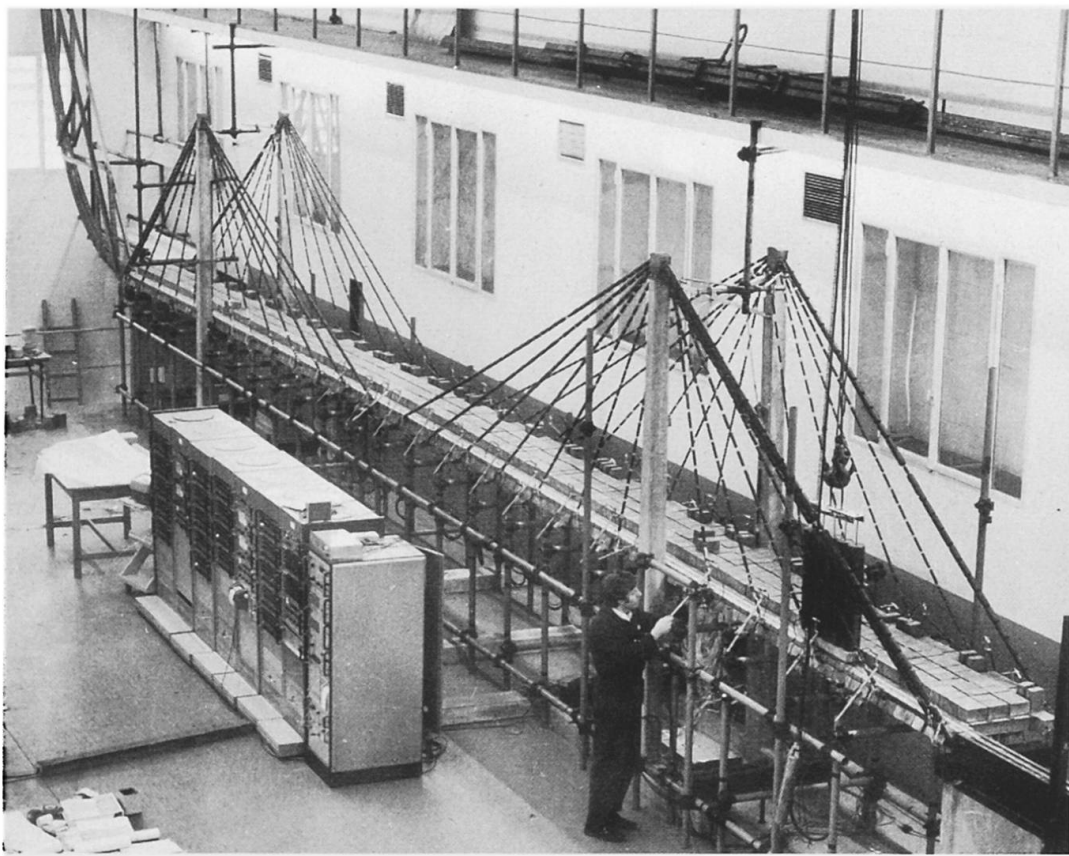


FIG. 10 1:33 scale model of road and railway guyed bridge over the Rio Paraná, Argentina, (complex steel structure). Statical and dynamic tests (running through of a train).

**Application of Precast Reinforced Concrete and Steel for Long Span Highway Bridges.
Economical Considerations.**

Application du béton précontraint et de l'acier aux ponts routiers de grande portée.
Considérations économiques.

Spannbeton- und Stahlanwendung für die Autobahnbrücken grösseren Spannweite.
Wirtschaftliche Aspekte.

E. DUBROVA

Director of the Research Institute of Automatized
Systems for Planning and Control in Construction
Gosstroi of the Ukr.SSR
Kiev, USSR

I. GRAMOLIN

Assistant of Deputy Chairman
Gosstroi of the USSR
Moscow, USSR

Generally two materials - steel and prestressed precast reinforced concrete are used for long span highway bridges. Experience obtained in the USSR and other countries during construction and design of these bridges allows to determine an effective area of application for superstructures of different forms using as the main index - the cost per sq.meter of deck area. This envisages that the index takes into account:

- unit cost of bridge construction work accounting requirements in temporary auxiliary assembly facilities;
- unit cost of main constructions of superstructures of different systems;
- unit cost of main construction of piers corresponding to the chosen system of superstructures.

Thus, the index takes into account all factors such as: cost of material and the fabrication of superstructure and piers and cost of bridge erection.

It is interesting to note that technological factors have considerable impact on final cost of the bridge.

This research indicates that depending on the chosen erection method the cost of auxiliary assembly structures and facilities (piers, falsework, trestles, pontoons, etc.) approximates from 70 to 20 per cent of the cost of superstructures. Consequently

the wrong choice of assembly method can lead to the cost of superstructures erection being equal to the cost of main construction.

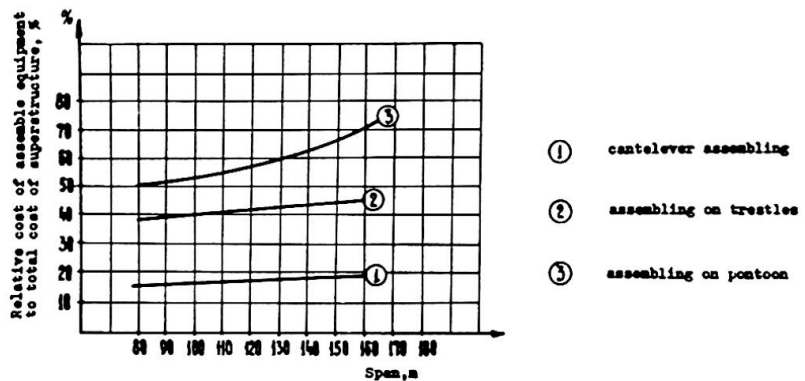


Fig. 1 Relation of assembly equipment and total cost to span of the bridge

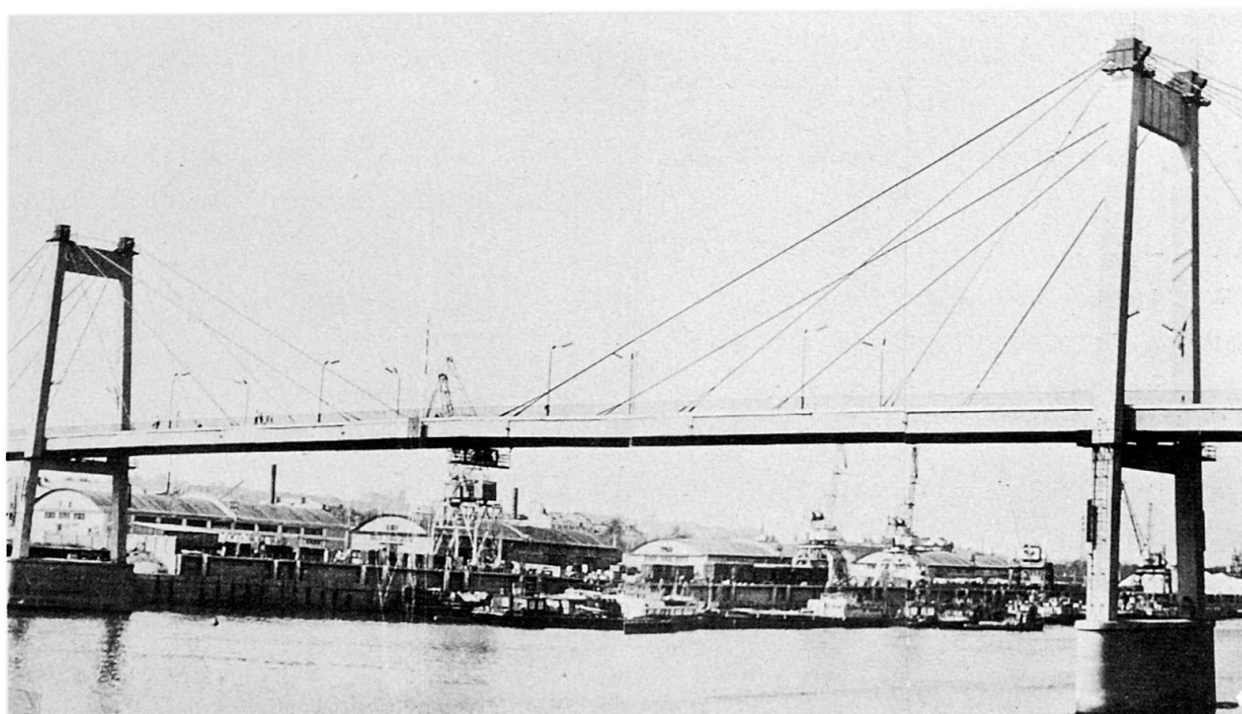
Figure 1 shows graphs of dependence of assembling facilities relative cost upon the cost of main constructions of superstructures of bridges with different spans. Most of the large bridges in the USSR are being erected this way due to the evident technological and economic advantages of cantilever assembly method.



The analysis of the main constructions cost included a review of the most promising superstructures:

I. Reinforced concrete bridges: continuous, rigid-frame cantilever, arch cantilever (Fig.2), arch, cable stayed (Fig.3), rigid-frame suspension (Fig.4).

II. Steel bridges: continuous girder, arch, cable stayed, suspension.



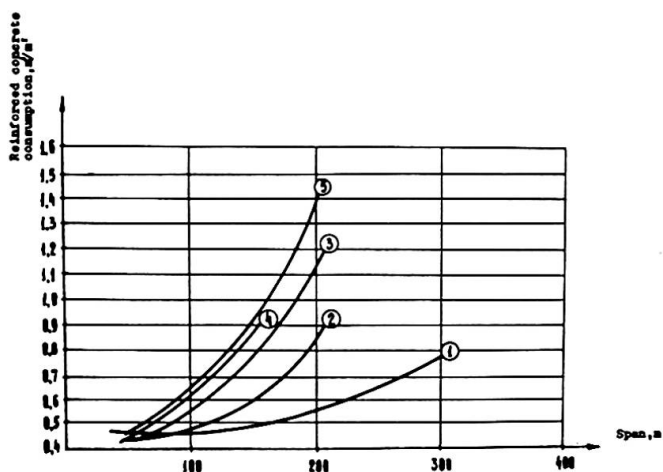


Fig. 5 Relation between reinforced concrete consumption and span of the bridge

consumption only for superstructures without respect for the consumption of material on piers can lead to serious errors while evaluating the chosen structure. The proposed approach to the evaluation of the economic effectiveness of various bridge systems made of steel and reinforced concrete is not expressed by the comparison of the steel and reinforced concrete consumption as a whole,

The consumption of steel and reinforced concrete per 1 sq.m of superstructures of various systems is shown in Fig. 5 and Fig. 6. The curves are drawn in accordance with the minimal consumption reached in practice of designing and construction. Then the specific material consumption for the bridge piers of various systems (Fig. 7) was analysed, because the account of material

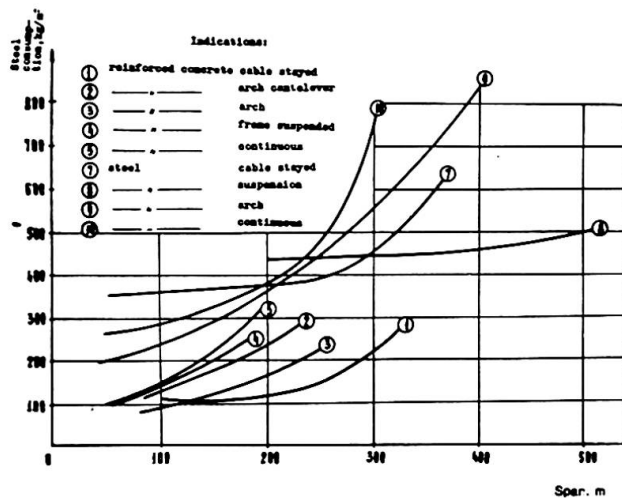


Fig. 6 Relation between steel consumption and span

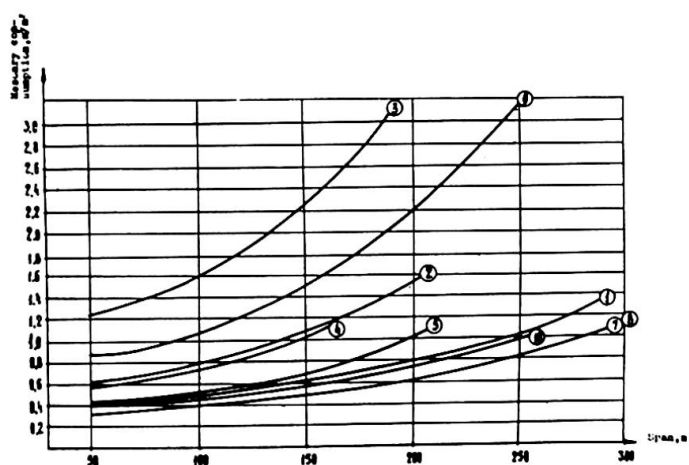


Fig. 7 Relation between masonry consumption and span

but is revealing the area of rational application of each system based on the comparison of certain specific consumption of materials for structural elements depending on spans and the real unit cost of these elements which takes into account the expenses both for manufacturing and erection of structures.

As a result of this analysis a graph was made for the unit cost per sq.m of various steel and reinforced concrete bridges. It includes the costs of construction of superstructures and piers and auxiliary assembly structures and facilities (Fig.8).

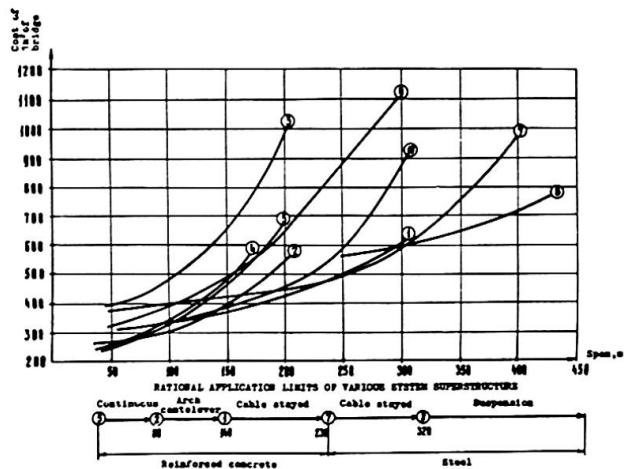


Fig. 8 Relation between cost of 1 m² the bridge and span

It's seen from the graph that at present, under the existing real prices one can speak about the rational application of reinforced concrete bridges of certain most effective systems with spans up to 230 m. These are the following:

- continuous superstructures with box girders erected by the cantilever method with spans from 50 to 100 m made of prestressed concrete;
- arch cantilever structures erected by the cantilever method with spans from 80 to 150 m made of prestressed concrete;
- cable stayed superstructures with the reinforced concrete rigid girder erected by the cantilever method with spans up to 140-150 m.

Then comes the area of the application of various steel bridges-cable stayed and suspension ones.

Naturally the local conditions of construction can considerably influence the definition of the rational application of the above systems. Thus, the availability of works located close to the surface or the construction of single-span bridges over deep canyons will require an additional study of the possibility to use thrust systems, since the volume of materials to be used for piers under these specific conditions is sharply reduced.

For example, when bridges are erected under conditions of city development where the construction of high access is not expedient, the structures of continuous girder or cable stayed bridges of small structural height are preferable.

The proposed method for the evaluation of the economic effectiveness of systems does not exclude real local conditions which are quite different from those mentioned in the present article, but on the contrary, it takes them into due consideration. For the overwhelming majority of bridge superstructure erected under the conditions of plain rivers with soft soils it is reasonable to continue persistent work at the modification and development of the most perspective reinforced concrete systems using them for spans up to 250 m.

SUMMARY The article presents method of choosing the area of rational application of bridges with reinforced concrete and steel span structures of various systems. It considers both the cost of main bridge structures (superstructures, piers, etc.) and the cost of assembly works, accounting necessary temporal structures (falseworks, pontoons, etc.). Cost index per sq.meter of deck area is used as effectiveness criterion.

RESUME L'article présente la méthode de la détermination d'application rationnelle des ponts en béton armé et en acier des systèmes différents. On y tient compte du coût des constructions principales du pont telles que la superstructure et les piles aussi bien que du coût des travaux de montage y compris les ouvrages provisoires (piles provisoires, coffrage, pcntons, etc.) Comme le critère d'efficacité on utilise l'index du coût d'un mètre carré du tablier du pont.

ZUSAMMENFASSUNG Im Beitrag wird die Methode der Bestimmung der rationellen Anwendung der Brücken mit Stahlbeton- und Stahl-Spannweitenbauten der verschiedenen Systemen beschrieben. Dabei wurden sowohl die Kosten der führenden Brückenkonstruktionen (Brückenspannungen, Stützen) als auch die Kosten der Montagearbeiten unter Beachtung der notwendigen Behelfsbauten (Baugerüst, Brückenschiff u.a.) berücksichtigt. Als Kriterium der Effektivität wird hier die Wertkennziffer eines Quadratmeters der Brückenfläche benutzt.